PRECISE DETERMINATION OF THE ^{76}Ge-^{76}Se ATOMIC MASS DIFFERENCE AND THE MAJORANA MASS OF THE ELECTRON NEUTRINO

A Thesis

Submitted to the Faculty of Graduate Studies

University of Manitoba

In partial fulfillment

of the Requirements for the Degree

Doctor of Philosophy

by

Jonathan Grant Hykawy

Winnipeg, Manitoba, Canada

May, 1991

ISBN 0-315-76902-5

PRECISE DETERMINATION OF THE ^{76}Ge-^{76}Se ATOMIC MASS DIFFERENCE AND THE MAJORANA MASS OF THE ELECTRON NEUTRINO

BY

JONATHAN GRANT HYKAWY

A thesis submitted to the Faculty of Graduate Studies of the University of Manitoba in partial fulfillment of the requirements of the degree of

DOCTOR OF PHILOSOPHY

ACKNOWLEDGEMENTS

I would like to thank my thesis supervisor, Dr. R.C. Barber, for his guidance, support and encouragement over the years that I have been associated with the Mass Spectrometry Group.

Many thanks should also go to Dr. K.S. Sharma for his support and for his many helpful insights into the study of physics, as well as his help with specific details and problems.

Over the years, I have worked with many other individuals, and I would like to thank all of them. Included in this list should be Mr. Clifford Lander, Dr. R.J. Ellis, Dr. G.R. Dyck, Mr. B.J. Hall, Mr. J.N. Nxumalo, Mr. P.P. Unger, and last, and in no way least, Mr. P. Beaudoin, a good friend whom I shall always miss.

My Canadian Union of Educational Workers sisters and brothers deserve special note. To Brenda Austin-Smith, Doug Torrance, Deb MacLatchy, Cathy Morgan and all the others, thank you for a wonderful time. And to my sisters and brothers in CUPE 1281, , especially Derek Blackadder, Bernie Lopko and Jim Keatings, you kept the union experience interesting.

I also would like to acknowledge the contribution of my high school physics teacher, Mr. Bryan Dentry, to my career. Without his showing me just how interesting physics can be at that early point in my life, I doubt I would have made it to this stage.

This work was supported by the Natural Sciences and Engineering Research Council of Canada. Their scholarship support allowed me to push ahead on research at times when it would have been impossible to do so otherwise.

To Jane Kitchen, for her support and for her wonderful presence during the time when I was scrambling to complete this thesis and preparing to defend it.

And, finally, I thank my family, especially my father John and mother Vicki, for all their help and their patience over the years.

Table of Contents

Table of Figures

Table of Tables

ABSTRACT

The double-beta decay process observed in ^{82}Se has been, until now, the rarest decay process ever observed in the laboratory. The lifetime has been measured to be of the order of 10^{21} years.

The postulated form of the double-beta decay known as the zero-neutrino mode, or $\beta\beta(0\nu)$, violates several of the principles of the Standard Model of physics. This decay form, applied to the candidate nucleus ^{76}Ge, would require the decay of two neutrons to two protons and the emission of only two electrons, violating conservation of lepton number and requiring the neutrino to be a Majorana particle. In addition, the neutrino would have to be massive and/or participate in a righthanded weak current process.

Since this decay would emit only electrons, its signature would be a characteristic sharp spike at the Q-value for the decay. There are currently a number of research groups searching for evidence of the $\beta\beta(0\nu)$ decay of ^{76}Ge.

Measurement by Ellis *et al.* in 1985 established the Q-value for the ^{76}Ge-^{76}Se decay. New measurements have cast some doubt on this determination, and, in the interests of resolving the controversy, a re-measurement has been made.

The new results of mass measurements on mass doublets in this area will be given. In addition, the implication of this new Q-value to the mass of the neutrino will be discussed. New limits on the neutrino mass will be derived.

1 Introduction

In mass spectroscopy a beam of ions is separated into components according to their mass so that either the mass (location) or the abundance (intensity) of these components can be determined. In instruments with sufficiently large resolving powers, the location is defined precisely and mass differences (and hence energy differences) between neighbouring nuclides can be measured with very high precision. These mass differences give the energy available for nuclear decays or reactions and reflect systematic variations in such properties as two-neutron separation energies (S_{2n}), thereby providing clues about nuclear structure.

Mass spectroscopy developed from the work of J.J. Thompson who measured the q/m (charge to mass) ratio for the electron [Th97]. Earlier, Goldstein had discovered positive rays (the *kanalstrahlen*) [Go86], and, subsequently, Wien [Wi98, Wi02] had measured their q/m ratio. The ratio for these rays was, of course, much lower than that for the electron.

In 1912, Thompson built a positive-ray parabola apparatus and used it to measure q/m ratios more precisely [Th12]. It was while using this device that Thompson found suggestive evidence for the existence of two isotopes of neon, ^{20}Ne and the much rarer ^{22}Ne. This was the result which essentially began the field of study we know of today as mass spectrometry. It was the first hint that separating ion beams by mass gave valuable clues about the isotopic nature of matter amongst the non-radioactive elements.

Mass spectroscopy is generally considered to have begun with the work of Aston [As19] and Dempster [De18], both of whom developed ingenious spectrographs. Both devices had severe limitations. The Dempster instrument used a 180° magnetic section which produced a direction focus (bringing to a focus ions which have the same mass but which enter the machine at slightly different angles) but did not produce a velocity focus (bringing ions

which have the same mass but which have different energies to the same place). The action of the instrument built by Dempster on an ion beam is analogous to the combination of a prism and a convex lens on a beam of light. In order to overcome the lack of velocity focus, Dempster's spectrograph required a monoenergetic source of ions. This could be achieved, for some chemicals, by using heated salts as a source material, but it limited the sample types used. In contrast, the Aston device had no ability to direction focus but did have a velocity focusing capability. A highly collimated beam was required in order to produce a well defined image. This restriction critically limited beam currents.

Aston used his instrument to establish roughly the whole number rule. He was the first to give unequivocal evidence among the light elements for the existence of isotopes, chemically identical substances with different masses. He also measured the isotopic composition of many elements, among them neon and chlorine.

Dempster [De20] also investigated the isotopic composition of many elements using his device, but the elements studied by Dempster were of a different chemical class than those studied by Aston. Dempster used his instrument to discover the isotopes of magnesium, and made isotopic abundance determinations of many elements, including zinc.

Aston [As23] also recognized that there were signs of divergences from the newly established whole number rule. Although the first serious investigations of this matter were made by Costa [Co25], it was Aston, with his second spectrograph, who made the first systematic study of nuclear binding. He chose ^{16}O as the mass standard and introduced the packing fraction:

$$packing\,fraction = \frac{M - A}{A}$$

as a measure of these divergences.

Somewhat later, Bainbridge, using his new device [Ba33], measured the masses involved in the reaction $^{1}H+^{7}Li \rightarrow 2^{4}He$, and provided thereby the first experimental evidence confirming Einstein's mass-energy equivalence relation [Ei05].

Until the early 1930's, specialized calculations were used to show that a particular geometry produced a direction or velocity focus. The first general description of focusing conditions were given by Herzog [He34] and by Mattauch and Herzog [Ma34a]. These equations incorporated into a single formalism all of the previous special cases. Further, they made possible the design of instruments for which the velocity and direction foci coincide, the much desired double-focusing instruments. Thus, these general focusing equations were crucial in elevating the mass spectrometer to a vital and general research tool.

On the basis of the work of Mattauch and Herzog, a state-of-the-art instrument was designed and built by Nier in 1935 [Ni40], its construction serving to mark the beginning of the modern era of mass spectrometry. It incorporated the newest techniques for vacuum systems, source construction and ion detection, the latter employing electrical rather than photographic means. Shortly thereafter, Dempster [De35], Bainbridge and Jordan [Ba36] and Mattauch and Herzog [Ma34b, Ma36] designed and built double-focusing instruments, incorporating the latest features of design and equipment.

With this new generation of double-focusing instruments a substantial increase in resolving powers became available. This allowed smaller mass differences to be resolved and studied. Additionally, since precision improves linearly with resolving power, the precision obtained by the new mass spectrometers was far superior to that obtained with the

older instruments.

The aberration in the image for an ion beam passing through both an electric and magnetic field in tandem can be expressed as a power series:

$$y_B = r_m\{B_1\alpha_e + B_2\beta + B_{11}\alpha_e^2 + B_{12}\alpha_e\beta + B_{22}\beta^2\}$$

where α_e represents a measure of the angular divergence of the ion beam and β represents the energy spread in the beam.

In this expression, $B_1 = 0$ means that the instrument produces a direction focus while $B_2 = 0$ corresponds to the production of a velocity focus. In the mid-1950's, several large instruments incorporating partial second-order focusing were proposed and constructed. Until then, instruments were double-focusing only to first-order. Instruments were designed with geometries which had the coefficient of $\alpha_e^2 = 0$ (*ie.* second-order direction focus). More recently, instruments have been designed which incorporate beam optics which eliminate all unwanted terms to second-order in the expansions, rather than only first-order. Second-order double-focusing instruments are currently preeminent in deflection-type machines. Work continued on the second order theory up to about 1980.

The mass spectrometer used to acquire the data in this work, Manitoba II, is based on one of many designs given by Hintenberger and König in 1959 [Hi59]. These designs emerged from early second-order theory in which the simplifying assumption was made that both electric and magnetic fields terminate abruptly. Improved calculations by Matsuda [Ma76] show that the effect of the actual fringing fields are slight, yielding small second order coefficients. Additionally, the third order coefficients were assumed to be small and, hence, third order effects were assumed to be insignificant contributors to the image aberrations. Manitoba II was constructed during the period 1964-1967, with operation com-

mencing in 1967 [Ba67, Ba71]. The instrument has been gradually improved ever since. For mass determinations it is the most precise deflection-type instrument in the world, having achieved a precision of better than 9 parts in 10^{10} [Si90]. This precision compares favourably with methods of determining directly the energy for nuclear reactions and decay Q-values.

Recently developed techniques in which ion traps are used suggest the possibility that even higher levels of precision may be reached in the future. These instruments, called ion cyclotron resonance mass spectrometers, or ICR-MS, incorporate, as a key element, superconducting magnets to provide extremely stable, uniform fields with very high field intensities (in excess of 5 Tesla). In ICR-MS, ions are trapped in the combination of an electric field, formed by a hyperboloidal electrode arrangement, with the intense magnetic field applied parallel to the axis of symmetry. When an RF pulse is applied, the ions in the trap move in a circular path in the magnetic field. In principle, if the field strength is known and the cyclotron frequency of the ion is measured, the mass can be derived very precisely.

In practice, there have been some problems in accomplishing this. Ideally, mass differences may best be studied by ICR-MS when both species are placed in the trap simultaneously and the frequency difference is used to derive the mass difference. In this case, however, the ions tend to circulate in such a way that they "beat" against one another, producing an effective frequency and causing the different ions to couple their motions. This introduces systematic errors which are difficult to remove, as there may always be some contaminant ions in the trap, even if only those which have evaporated from the trap itself.

The above effects arise almost entirely from the presence of more than one species of ion in the trap at a given moment. Most of these effects can be avoided by having only one ion in the trap during a measurement. This mode of operation, known as single-ion cyclotron

resonance mass spectrometry, or SICR-MS, has arisen in an attempt to have the ion trap realize its full potential for mass measurement. Some of the SICR-MS units use a SQUID to detect the ions as they move about the trap. RF pulses are used to eject sequentially ion after ion until only one remains in the trap. The cyclotron frequency is then measured until the ion collides with a neutral atom or until another ion enters the trap. The limit on precision for the mass difference as measured by such a device is estimated to be as small as a few parts in 10^{12} [Co89], but recently questions have been raised about the uncertainty associated with other factors necessary to achieve the stated precision, as well as the certainty with which systematic effects have been removed. For example, obtaining such high precision in the final result requires that the ion in the instrument travel the same path, repeatedly, to better than one part in 10^6. Also, there can be no charges on the inner surface of the instrument which perturb the fields to greater than the same high precision as that achieved in the final measurement. Both these conditions are extremely difficult to achieve. The most precise SICR-MS measurement to date is that reported by Cornell *et al.* [Co89] for CO-N_2.

While precise mass differences from mass spectrometry, as described in this thesis, give nuclear reaction and decay Q-values, these are also determined by direct energy measurements. In general, the precision of the mass spectrometric data compares favourably with the best reaction data.

The reaction technique which most closely rivals mass spectrometry in precision is the (n,γ) method. In this technique, a nucleus absorbs a thermal neutron and then de-excites to the ground state by emitting a gamma ray. The gamma ray energy, typically several MeV, can be measured very precisely, normally to levels of around 0.5 keV.

Other reactions commonly used include the (d,p), (α,d) or (t,p) with somewhat lower

precision, typically on the order of a few keV. For certain α decays, the energy of the α particle has been determined to better than 1 keV, although for most α decays the precision is much lower.

Experiments such as those described above involve nuclides on or near the line of beta stability. These experiments have been extended to study nuclides well removed from this region. In instruments such as ISOLDE II at CERN or the Chalk River On-Line Isotope Separator (Chalk River ISOL) [Sc81] unstable atoms are produced by bombarding a target with heavy ions (^{14}N) and subsequently ionizing the unstable atoms produced by the bombardment. For example, Mo targets enriched in ^{92}Mo can be bombarded by a ^{14}N beam, producing ^{102}Cd. These exotic, short-lived ions are then passed through a mass analyzer. While the precisions attained by these instruments are lower than those obtained by conventional mass spectrometers, useful levels of precision, of the order of tens of keV or several parts in 10^6, are obtained. These devices may be used to study nuclides having half-lives of only seconds or even less. Such studies are directed at the nature of nuclear systematics for isotopes well removed from the line of beta stability and are required for the testing of models for nuclear masses.

This thesis is directed at the mass difference (*i.e.* the energy available) for a rare decay involving two nuclides near stability and utilizes conventional high resolution mass spectrometry. The isotope ^{76}Ge must decay because it is not the most tightly bound isobar at A=76. ^{76}Ge should decay to ^{76}Se (see Figure 1-1). However, it cannot proceed by sequential single beta decays because these would require a decay from ^{76}Ge to ^{76}As, a decay which is not energetically possible. The decay may proceed, however, by the very rare double-beta reaction. This can be accomplished by either of two modes, either the two-neutrino or zero-neutrino:

$$^{76}Ge \rightarrow {}^{76}Se + 2\beta^- + 2\bar{\nu}$$

$$^{76}Ge \rightarrow {}^{76}Se + 2\beta^-$$

The two-neutrino mode is more likely to exist at first glance. It conserves lepton number and does not contradict the standard model in any way. However, the zero-neutrino mode has the advantage that only two product particles are emitted. If one examines the integrals related to the production of two versus four particles, one finds that the phase space for the production of two particles is much more favourable and will occur more rapidly than will the production of four particles. Hence, the zero-neutrino mode has a significant phase space advantage and, theoretically, a much shorter half-life. This mode requires that the neutrino be a Majorana particle [Ma37].

Single beta decay was studied by many scientists in the 1930's. The decay was originally presumed to be of the form:

$$(A,Z) \rightarrow (A,Z \pm 1) + \beta^{\mp}$$

and, on this basis, the emitted β particle would be expected to have a well-defined energy. This was not the experimental result. Instead, the electrons had a continuum of energies, a fact suggesting at least one additional product particle, although such a particle had not been seen in any experiment. Pauli [Pa33] postulated the existence of a neutrino and Fermi [Fe34] incorporated this "ghost" particle in his quantum mechanical description of the decay. Further work has shown the neutrino to be very light, and, in fact, the neutrino has long been considered to be massless. Moreover, it has a very low cross-section of interaction with matter.

The standard particle model, based on the SU(5) group, was developed over the course of many years. One of its postulates is that all neutrinos are massless. A massless neutrino

gives a solution of the Dirac equation which has a definite helicity. Experimentally, the neutrino is a left-handed particle and the anti-neutrino is right-handed. There are no right-handed neutrinos. This breaking of symmetry would mean that the double-beta decay would proceed only by the two-neutrino mode.

Some of the newest theoretical work on unification of the fundamental forces of nature raises questions about the SU(5) model. SU(5), with an enlarged particle content, has a configuration which generates non-zero neutrino masses [Ze80]. SO(10) contains massive neutrinos as a matter of course. Aside from the 5-dimensional and 10-dimensional descriptions of particles contained in the SU(5) model, SO(10) also contains an extra neutral fermion which may be interpreted as a right-handed neutrino. The existence of such a righthanded neutrino would mean that the zero-neutrino mode of double-beta decay could occur.

Accordingly, experimental work to investigate neutrino mass has become a matter of renewed interest and activity in physics research. An experiment which is sensitive to neutrino mass is the observation of neutrinoless double-beta decay and the determination of the corresponding half-life. Measurement of the half-life for neutrinoless double-beta decay allows the calculation of the electron neutrino mass by one of several relationships between $T_{1/2}$ and $\langle m_{\nu_e} \rangle$. For example, the relation given by Grotz and Klapdor [Gr85]:

$$\langle m_{\nu_e} \rangle^2 \approx \frac{2.5 \times 10^{23}}{T_{1/2}} (\text{eV})^2$$

If the zero-neutrino decay occurs, the escaping electrons would carry all of the available energy. This means that the energy spectrum will show a sharp peak at the Q-value of the decay. Moreover, Ge is a uniquely favourable material since it can be formed into well characterized detectors. ^{76}Ge thus serves both as a potential double-beta decay candidate

and as its own detector.

Groups are currently studying the energies of decays in a hyper-pure Ge crystal [Av86]. These studies require the energy available for the double-beta decay of ^{76}Ge; it is here that mass spectrometry makes its contribution. In 1985, Ellis *et al.* used the Manitoba II instrument to determine this Q-value [El85]. Further improvements to Manitoba II, specifically (a) in data acquisition and analysis, (b) in the stability of the magnetic field, and (c) in the instrumental resolving power, as well as some troubling discrepancies in relating the measurements of Ellis *et al.* and recent (n,γ) data prompted a redetermination of the ^{76}Ge-^{76}Se mass difference.

Figure 1.1 Mass Parabolae for A=76

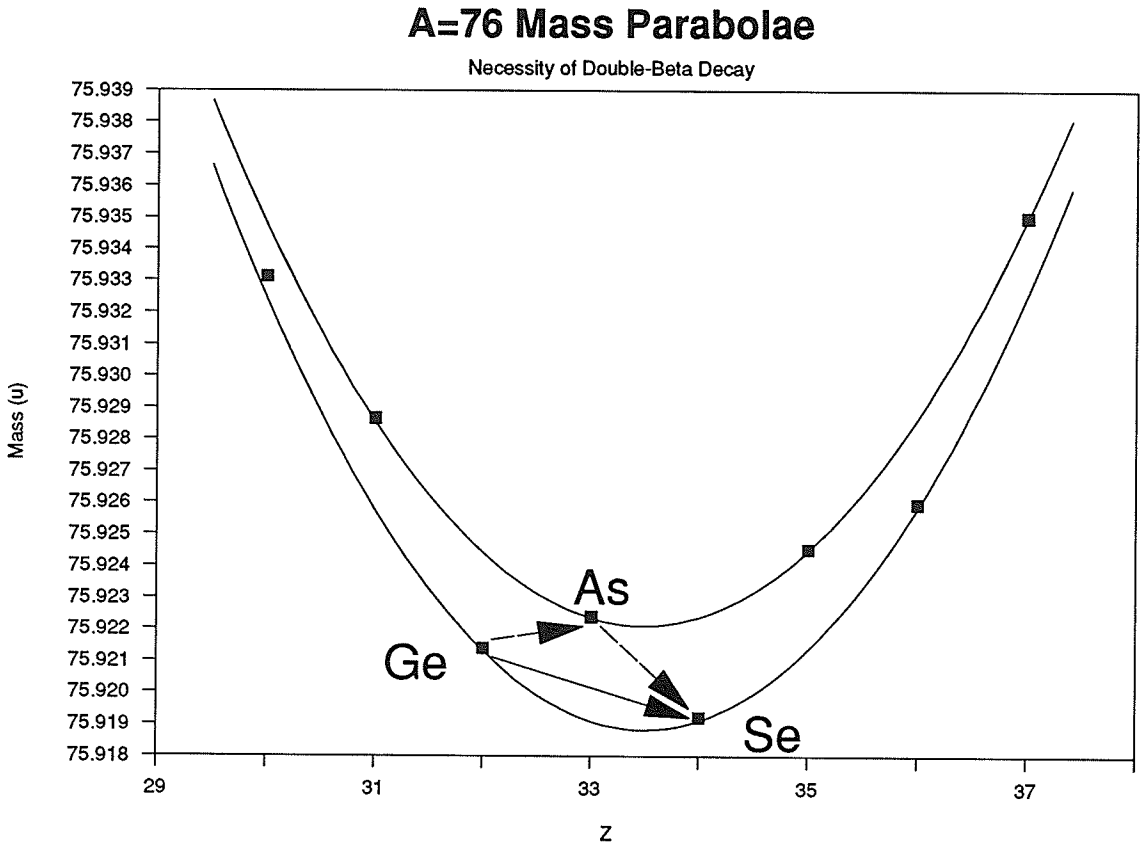

2 The Neutrino Mass Problem and ^{76}Ge-^{76}Se

2.1 The Neutrino and Neutrino Mass

The neutrino was proposed as a hypothetical particle, required to explain the discrepancy in the electron energy spectrum for single-beta decay seen in the early 1930's [Pa33, Fe34]. At that time, the single-beta decay was thought to produce only the beta particle and daughter nucleus. The beta particle should then carry away almost all of the available energy and the plot of the energy spectrum of the emitted beta particles should be a sharp peak at the Q-value. Experimentally, the shape of this plot was a broad curve, indicating the presence of at least one other product particle. Without the presence of this particle, energy could not be conserved in the single-beta decay. Fermi included this particle, which had not been observed in any experiment conducted up to that time, in his quantum mechanical description of the single-beta decay. He assumed that the neutrino was massless, and, until recently, that assumption has been retained. Even the current SU(5) model includes a massless neutrino, having zero charge and magnetic moment and no internal structure. The neutrino has a very low cross-section of interaction with matter. The standard model includes three neutrino flavours, one corresponding to each of the charged leptons; electron, muon and tauon neutrinos. These so-called flavours are conserved in reactions.

The neutrino served to resolve the problem of non-conservation of energy in beta decay. It is now being invoked to help explain away other problems as well. Research on the rotational rates of galaxies and star clusters would suggest that the amount of matter in existence taken as a ratio with the amount of matter needed to just close the universe gravitationally is very close to one [Fi82]. However, the observed levels of luminous matter give a ratio of only about 0.01. It seems that the universe contains a great deal of dark matter not visible to us here on Earth.

This matter might be in the form of dust or in even more exotic forms, such as brown dwarf stars, black holes or gravitinos [Tu82, Si82]. However, nuclear and particle physics admits an even stranger possibility as most likely. Stars produce a huge number of neutrinos and anti-neutrinos. When the neutrinos escape the star they go out into the universe at large and, since they do not interact often, there is a very large number of neutrinos travelling through space. If these particles have even a very tiny mass, there could be a huge amount of matter present in a neutrino cloud about each star and each galaxy. This cloud would be undetectable.

Massive neutrinos might answer one of the fundamental problems in cosmology and astrophysics. However, they might also serve to answer one of the more perplexing problems in theoretical physics as well.

Current theory, in the form of the standard SU(5) particle model, postulates that the neutrino is massless and that the weak force maximally violates symmetry by coupling only to left-handed neutrinos or right-handed anti-neutrinos. However, the most promising new theories dealing with grand unification predict that the neutrino will be massive and that the violation of symmetry by the weak force will not be maximal. Instead, the weak force will be composed of both left- and right-handed currents, capable of acting on both left- and right-handed neutrinos. These theories work quite well in some respects, but there is currently no evidence for such a weak force and no evidence for a massive neutrino. If a non-zero neutrino mass were verified, it would not necessarily follow that the newer unification theories are correct. However, experimental evidence regarding the question of neutrino mass clearly places important constraints on acceptable theory.

The neutrinoless double-beta decay may be the most sensitive experiment currently available for detecting a massive neutrino or parity mixing neutral currents. This decay will

only proceed if the neutrino has a mass or the weak current has a right-handed component.

If a pure Ge crystal is used as a highly sensitive detector, one should be able to see the decay products from the double-beta decays of ^{76}Ge. The two-neutrino decay modes involve emission of two anti-neutrinos and two electrons. Since the anti-neutrinos will not be detected, only the energies of the electrons will be noted. The energies for these decays will lie on a curve which has a zero at both the origin and at the Q-value. The neutrinoless double-beta decay mode involves the emission of only the two electrons. Since both electrons will be detected, and they carry all of the energy of the decay (apart from a small amount of energy taken up by the recoiling daughter nucleus), their energy spectrum will be a sharp peak at the Q-value. If it can be established that this peak is present, then the neutrinoless double-beta decay has been observed and a half-life can be determined for the second of the two processes pictured in figure 2-1, viz.:

$$^{76}\mathrm{Ge} \rightarrow {}^{76}\mathrm{Se} + 2\beta^{-}$$

The existence of this neutrinoless decay mode would indicate an inadequacy in the SU(5) model. At present, five groups [Av86] are actively observing pure Ge crystals and are searching for evidence of decays in ^{76}Ge with an energy of 2040.71 keV, the Q-value measured by Ellis *et al.* [El85] using Manitoba II.

The neutrinoless double-beta decay proceeds if the neutrino is a Majorana particle. The neutrino and anti-neutrino are equivalent in the Majorana [Ma37] representation. The Majorana view differs from the Dirac view only if the mass of the neutrino is non-zero. A solution of the Dirac equation for a neutrino mass of zero gives a solution which has a definite helicity. Experimentally, the neutrino seems to be left-handed, having a Dirac

equation solution of the form $[1-\gamma^5]u_\nu$. Anti-neutrinos are right-handed with a solution of the form $\overline{\nu}_\nu[1+\gamma^5]$. There is currently no evidence for right-handed helicity states of the neutrino.

In other experiments evidence for a non-zero neutrino mass is being sought. One of the most promising of these depends on the shape of the Kurie plot for the beta decay of ^{3}H. If the neutrino were massless, the curve of electron energy would be a continuum ending at exactly the Q-value for the decay, the energy difference between ^{3}H and ^{3}He. If the neutrino were massive, the end-point of the curve would differ from the Q-value by an amount corresponding to the neutrino mass. Fitting a theoretically derived curve to the data near the endpoint of the electron energy data allows one to derive both the experimental endpoint and the deviation from the Q-value, and hence the neutrino mass. In order to accomplish this, one requires sufficiently precise knowledge of the shape of the electron energy spectrum and of the Q-value.

There have been reports of non-zero masses from such work. The ITEP group reported a mass of $17eV < \langle m_{\nu_e} \rangle < 40eV$ [Bo87]. However, recent measurements are inconsistent with this range, and the ITEP result is doubted at this time.

Simpson, on the basis of a deviation in the endpoint of the ^{3}H decay spectrum, has suggested the existence of a very massive electron neutrino of 17.1(2) keV [Si85]. Very recently, two other groups have reported the possible effects of very massive neutrinos in the Kurie plots from other beta decay sources.

The current best upper limit from this type of work is that of Bowles *et al.* [Bo89], *viz.* $\langle m_{\nu_e} \rangle < 13.4eV$. They caution that, mathematically, their data actually suggests a negative value for the mass and that small, positive masses would give such data only 8% of the time.

Geochemistry provides a complementary check on neutrino masses. Studying the ratio of the double-beta decay rates of ^{130}Te and ^{128}Te by examining the concentrations of ^{130}Xe and ^{128}Xe in tellurium ores, Kirsten *et al.* [Ki83] report a limit on the electron neutrino mass of $\langle m_{\nu_e} \rangle < 0.44eV$ and $\eta < 2.4x10^{-5}$ at the 95% confidence level.

Another interesting source of data is that of the supernova SN1987a. Neutrino observatories which were recording data the night on which the blast from this object reached our world were able to record many neutrino events, probably created when electrons were crushed into their nuclei and the parent star turned into a neutron star. Bahcall and Glashow [Ba87] find $\langle m_{\nu_e} \rangle < 11eV$ given the time lag between first and last neutrinos in the burst of events associated with the supernova. If neutrinos were massive, one would expect that the first neutrinos to arrive would be those with the highest energy. There is no such ordering evident in the data. A model-independent analysis [Ko87] of the neutrinos detected and their energies gives a result of $\langle m_{\nu_e} \rangle < 20eV$.

These neutrino events of SN1987a can be classified as to their mass, given some assumptions about the mechanism of production of these events. In the most optimistic of these papers, Cowsik [Co88] gives data which suggest two mass "families" of neutrinos were emitted from the supernova. One group had a mass of about 4 eV, the other a mass of about 22 eV. While the masses given are non-zero, the results must be regarded as highly conjectural.

Figure 2.1 Two-Neutrino and Zero-Neutrino Double-Beta Decay

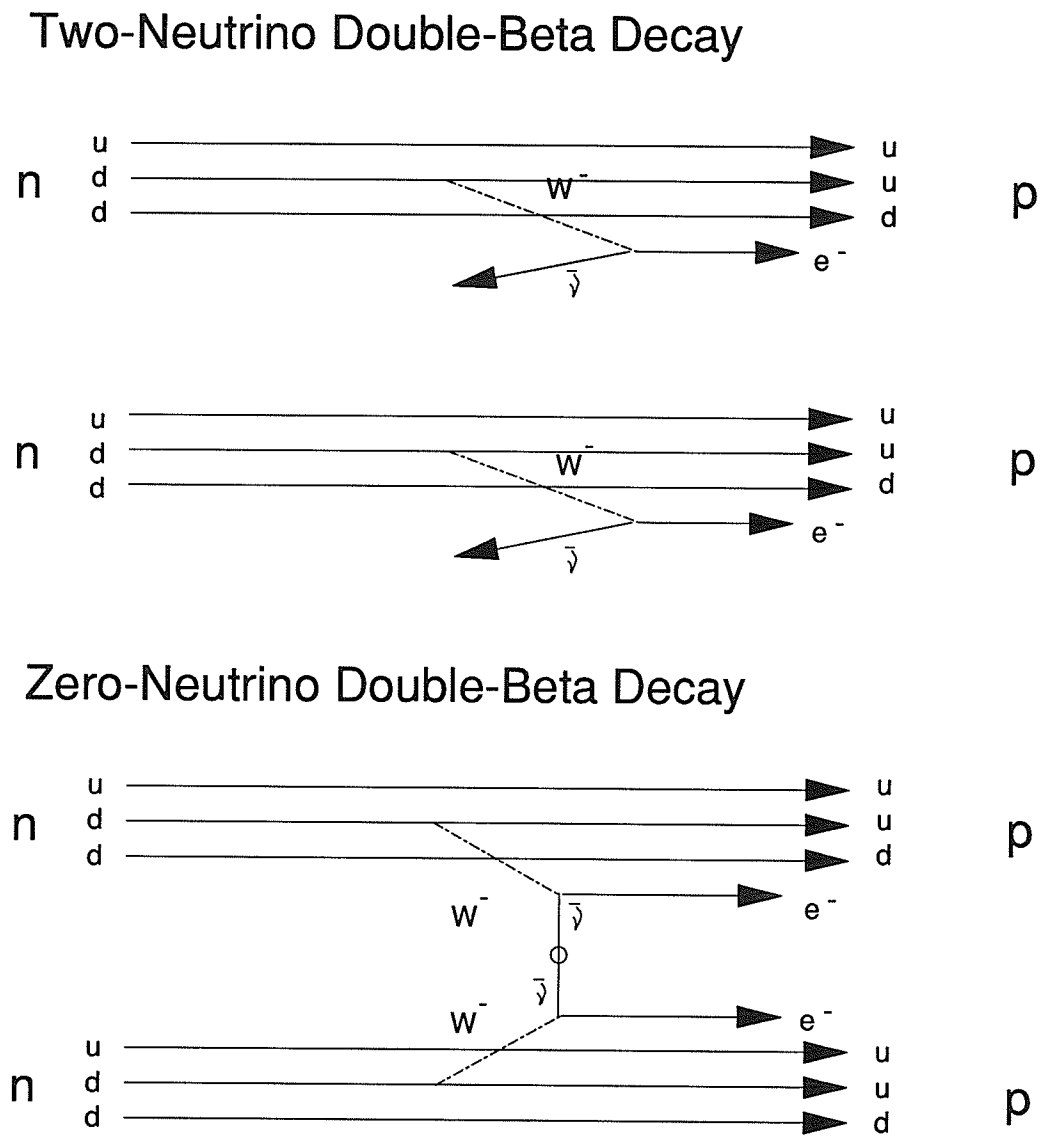

2.2 The Result of Ellis *et al.*

In 1985, Ellis and his co-workers measured the value of the mass difference between ^{76}Ge and ^{76}Se, as well as other related mass differences which overdetermine the final result [El85]. The value thus obtained was 2040.71(52) keV. This value has since been used to examine the spectra from experiments searching for the neutrinoless double-beta decay of ^{76}Ge. In Ge crystals, there have been no statistically significant events at the Ellis Q-value. The smallest upper limit, based on the Ellis value, is given by the ITEP group of Vasenko *et al.* [Va90] with $\langle m_{\nu_e} \rangle < 0.46eV$.

The Ellis value comes from a set of data combining measurements on both metal and single chloride doublets. The data taken include values which can be used to calculate the two-neutron separation energy (S_{2n}) for certain isotopes. Two of these impact directly on the measurement of ^{76}Ge-^{76}Se. However, these values, as tabulated below, are in very poor agreement with the S_{2n} energies determined from reaction data, specifically some new (n,γ) [Hu89] measurements:

Table 2-1

Nuclide	S_{2n} (keV)		
	Ellis *et al.*	(n,γ)	References
^{74}Ge	16983.21(61)	16978.5 (13)	Wa85, Hu89
^{78}Se	17919.50(79)	17916.7 (3)	En81, Yo85
^{76}Ge	15939.74(69)	15933.9 (10)	Wa85

The poor agreement between these values is unusual and disturbing, especially given the historical accuracy and agreement between these two techniques.

The Q-value can also be compared to the graph of energies from the USC/PNL experiment of Avignone *et al.* [Av85]. The Q-value measured by Ellis *et al.* suggests no neutrinoless decay events and hence gives only an upper limit on the neutrino mass. This in itself would not be considered strange. However, Avignone *et al.* note a statistically significant peak at 2044.72 keV in their spectrum. They discuss the possibility that, if there were a systematic error in the value given by Ellis *et al.* which shifts this value to 2045 keV, then the neutrino might be shown to have a mass. At the time, there was no other explanation for this peak in the decay data. In a later paper [Av86], Avignone *et al.* withdraw their claim for a statistically significant peak at 2044.72 keV.

The importance of this Q-value in interpreting the spectra used to search for the rare neutrinoless double-beta decay prompted us to remeasure the ^{76}Ge-^{76}Se mass difference. This present series of measurements was intended to re-determine the Q-value to higher precision and, incidentally, to confirm that systematic effects had not been introduced inadvertently during the recent modifications made to the Manitoba II spectrometer.

3 Manitoba II

3.1 The Manitoba II High Resolution Mass Spectrometer

Manitoba II has been described extensively elsewhere [Ba67, Ba71]. It is nominally a 94.65° electrostatic analyzer with 1.00 m radius followed by a 90° electromagnet with 63 cm radius (see figure 3-1). The design is one of the second-order double-focusing arrangements proposed by Hintenberger and Konig [Hi59] on the basis of a calculation in which the fringing fields are assumed to terminate abruptly. Subsequently more elaborate and realistic calculations by Matsuda have shown that, for Manitoba II, the effect of the fringing fields on the second-order coefficients remains very small [Ma76].

The original construction of Manitoba II was completed in 1967 but substantial improvements have been made since that time. The most recent major upgrade to the instrument has involved the (a) construction of new coils for the electromagnet and the replacement of the associated power supply, and (b) the rebuilding of the control and detection electronics, as described in the Ph.D. thesis of G.R. Dyck [Dy90].

The coils previously had approximately 1800 turns of heavy gauge copper wire and required relatively low current. The new coils, which have 24 turns of hollow-core copper conductor (cross-section 0.229" square, 0.128" inner diameter) through which deionized cooling water is pumped, can carry much higher currents. In this high current design, superior regulation of the magnetic field is achieved, and drastically improved stability of the peak position is obtained.

This has resulted in much easier operation. Moreover, this recent upgrade has made it possible to operate at higher resolving power, thereby significantly improving the associated precision.

The reconstruction of the control electronics has improved the reliability of operation.

The replacement of the electron multiplier with the present Galileo Electro-Optics Model 4830G prompted a complete analysis of the detector and resulted in an improvement in the efficiency of the detection system. An Amptek A-101 pre-amplifier replaced an older, custom-made pre-amplifier and resulted in a reduction in the deadtime of the electronics. This is described in the Ph.D. thesis of G.R. Dyck [Dy90] and below.

Manitoba II has two ion sources which are available, the choice of which depends on the chemical form of the desired sample and of the desired ion. The first is a modified Finkelstein type described by Barber *et al.* [Ba71], Bishop et al. [Bi69] and Meredith et al. [Me71] and used extensively in previous work. This source is shown in cross-section in fig. 3-2. The second is a duoplasmatron, described by Dyck [Dy90], and shown in fig. 3-3. For this work, the modified Finkelstein source was used exclusively.

In addition to the improvements described above, several improvements were made to the data acquisition system and to the software used to analyze the mass spectral data (see Section 3.2).

Figure 3.1 Manitoba II

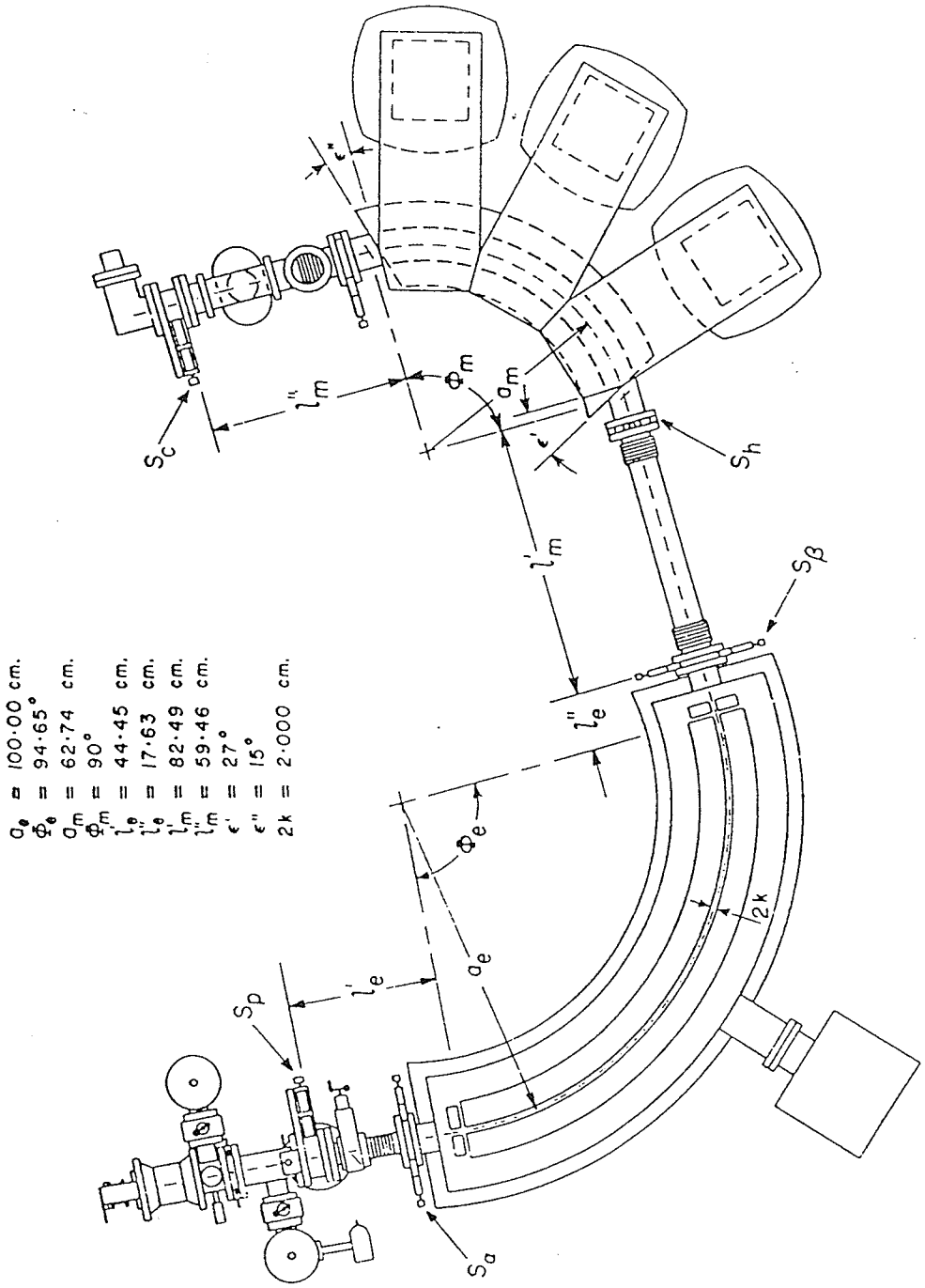

Figure 3.2 Modified Finkelstein Ion Source

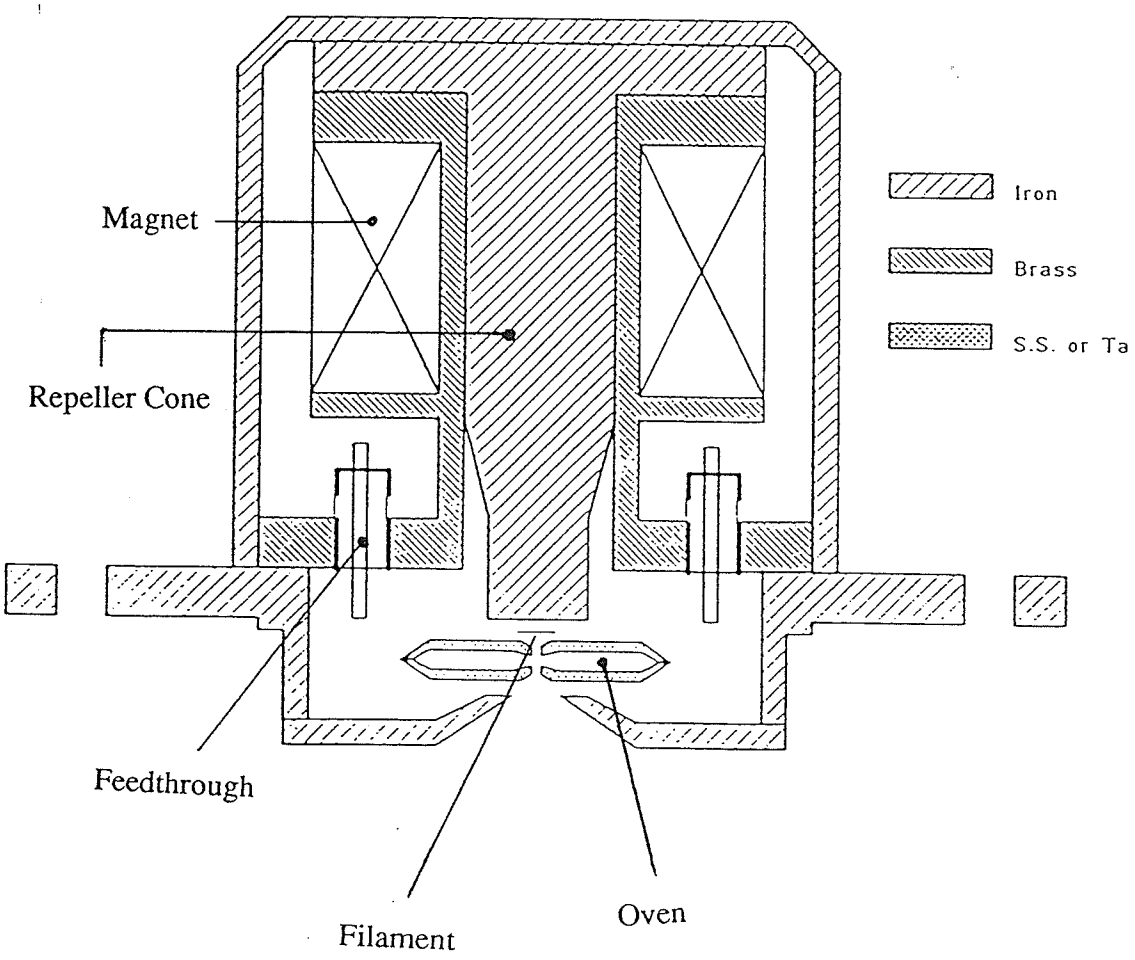

Figure 3.3 Duoplasmatron Ion Source

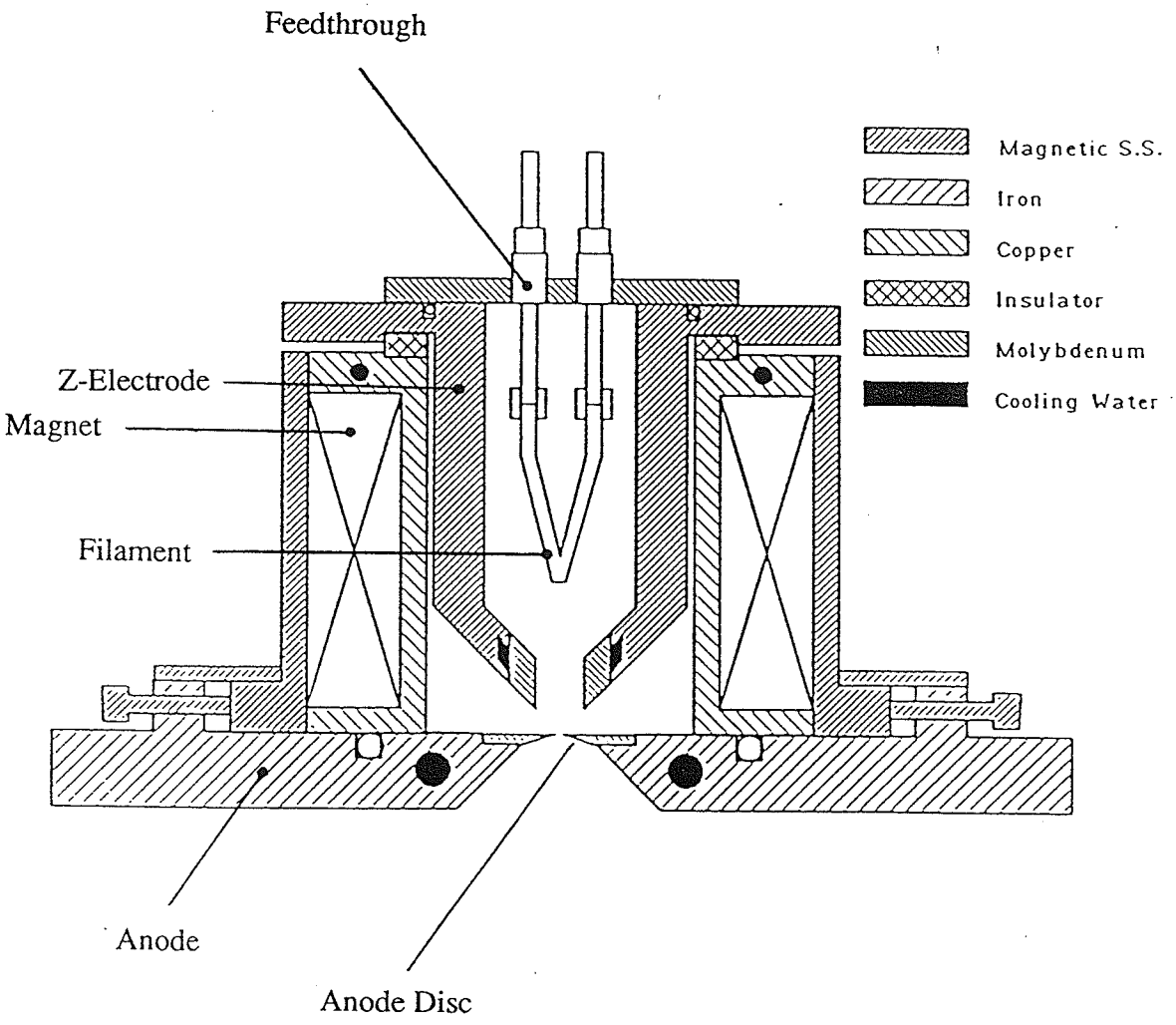

3.2 Data Acquisition and Analysis

The technique for measuring the mass difference of a doublet by a mass spectrometer depends on a theorem by Swann [Sw31] and by Bleakney [Bl36]. If we have two ion species of masses M and M′, where $\Delta M = M - M'$ and $M > M'$, and if we switch the voltages applied to all electrostatic lenses and elements within the machine as given by:

$$\frac{\Delta V}{V} = \frac{\Delta M}{M'}$$

while holding magnetic fields constant, then both mass species will travel the same path. This means that these different masses will strike the same point on the plane of the collector slit. While the paths traversed by the ions are relatively insensitive to most of the switched voltages on Manitoba II, the paths are very sensitive to the voltages applied to the plates of the electrostatic analyzer.

In the past, including the work of Ellis *et al.* [El85], measurements were made on the Manitoba II instrument by the visual null method of peak matching. This method has been described elsewhere [Ko79]. In this technique, the voltage applied to the plates of an electrostatic analyzer, V, is switched by a small amount, ΔV, through the action of an electromechanical chopper. Only one such switching voltage is necessary.

An ion beam, as introduced into the electrostatic analyzer of Manitoba II, has a uniform cross-section. The homogeneity of the beam profile is maintained until the beam reaches the detector end of the instrument. Once at the detector end, the ion beam is incident upon a detector slit. In order to generate a peak in the mass spectrum, a set of coils is used to sweep the ion beam across the detector slit. The current in this set of coils is provided by the output of a Kepco bipolar operational power supply/amplifier, the input signal to which is the sweep voltage of the oscilloscope monitoring the detector output. Thus, the sweep

of the ion beam and the sweep of the oscilloscope trace are synchronized.

The ion beam at the detector slit has a uniform profile. The detector slit is a pair of stainless steel jaws held a uniform distance apart. When the ion beam is swept across the slit and viewed on the live display, a mass spectral peak is generated. Should the ion beam and the slit both have the same width, the generated peak will be a triangular shape with an effective width twice that of either the incident beam or the slit. Should either the slit be wider than the beam or *vice versa*, the output of the detector will reach a maximum intensity and sustain that level for some period during the sweep of the ion beam across the slit. The mass spectral peak will not be a triangular, but will instead be "flat-topped", a triangle with the top point cut away. For maximum sensitivity, the detector slit should have the same width as the ion beam. Mass spectral peaks displayed on the live display should be sharp triangular peaks, rather than "flat-topped".

Counts are added to the memory of the multichannel analyzer (MCA) during the period the unswitched peak is on the live display and subtracted from the memory during the period when the switching voltage is applied and the switched peak is on the live display. By adjusting amplifiers so that the apparent heights of the two peaks on the real-time screen are equal, the switching voltage applied to the plates of the electrostatic analyzer can be adjusted until a match is achieved. This matched condition is indicated by a symmetric error signal on the screen of the oscilloscope connected to the MCA. Eight matches constitute a run, the eight matches corresponding to different voltage applications which serve to remove operator bias in the measurements.

In the visual null method, a run is completed more quickly than in the computer-assisted technique, which will be discussed in a subsequent paragraph. However, the visual null method does not have the advantage of retaining a permanent record of the data as the

computer-assisted method does. Further, the final level of precision achieved with the visual null technique cannot equal that achieved by the computer-assisted method. Moreover, use of the visual method makes it impossible to verify whether low-levels of contaminants are present, *a posteriori*.

The application of multichannel scaling (MCS) techniques was originally implemented for atomic mass determinations on a mass spectrometer by Benson and Johnson [Be66] at the University of Minnesota. The inherent advantage in using a MCS technique rather than a visual method is the improvement in the signal-to-noise ratio of the accumulated error signal. The fundamental reason for this improvement is the increased integration time over which ions are collected. An MCA with a greatly improved analog-to-digital converter was used on the Manitoba II mass spectrometer [Me72]. A variation on this approach was used by Bainbridge and Moreland [Ba60]. All data used in this work were acquired using the computer-assisted matching technique described by Meredith *et al.* [Me72].

At the heart of the computer-assisted matching system is an electromechanical chopper which applies appropriate voltages to the plates of the electrostatic analyzer. Four such voltages are used. These voltages are applied during the time that a signal averager is operating in the pulse counting mode and acquiring data on beam intensity at the collector slit. Figure 3-4 is a diagram which shows when voltages are applied relative to control pulses from the chopper.

The voltage displacements applied to the plates of the electrostatic analyzer of the spectrometer are nominally zero (corresponding to the unswitched peak), ΔV (corresponding to the switched peak being approximately coincident with the unswitched peak) and $\Delta V - \delta V$ and $\Delta V + \delta V$ (corresponding to the switched peak being slightly displaced to either side of the approximately matched condition). Each of the four peaks is stored in a quadrant of the

memory of the MCA.

These peaks are then subjected to two types of numerical analysis. The first type of analysis relies on a straightforward centroid technique, which determines the centroid location of each peak. By comparing the centroid of the peak in quadrant 2 to the centroids of the peaks in quadrants 0, 1 and 3, and then factoring in the switching voltage data, we can calculate the ΔV for an exact match. Since we have ΔV, we can use Bleakney's Theorem to calculate ΔM.

The second type of numerical analysis completed is a least-squares type. Experience with this method has shown it to be more robust and better able to handle such details as asymmetric peak shapes. The reference peak in quadrant 2 is taken and compared to each of the peaks in quadrants 0, 1 and 3. The peak from quadrant 1 is taken and subtracted from the reference peak in quadrant 2. Each difference is calculated, squared and stored, channel by channel, and a total is obtained, equivalent to the X^2 for the pair of peaks. Then the peak from quadrant 1 is artificially shifted by one channel and the process repeated to give a second point on the X^2 curve. This continues until sufficient data is accumulated to fit a parabolic curve to the X^2 data and find the minimum. The location of this minimum in channels corresponds to the actual offset for the quadrant. Each of the quadrants 0, 1 and 3 has an offset from the reference peak in quadrant 2 which is calculated in this fashion. The offsets are then associated with the appropriate switching voltages and a linear regression is used to find the "best" value for ΔV. Once again, ΔM is then easily derived.

The current technique of computer matching with Manitoba II uses the squares of the differences. In the past, the absolute values of the differences between quadrants was also used [So73]. Although there is no overriding theoretical reason to prefer one method over the other, the squares of differences are now used because this technique more closely

resembles the treatment of data in Gaussian statistics.

A comparison of the two procedures can be made with archived data. If we calculate the mass difference for a typical series of eight spectra (one run), the largest discrepancy between mass differences derived by the two different techniques occurred with the value 3212.55 ± 2.22 μu (from squaring differences, nine point quadratic fit) and the related value 3207.08 ± 2.42 μu (from absolute values of differences, nine point quadratic fitting). In general, the final mass differences calculated by the two methods for a given doublet (*ie.* averaging all data acquired) are equal to well within error.

Further, it has been shown that the method of squaring differences generally results in a reduced X^2 for a given doublet which is numerically nearer to one than that which results from the method of absolute values. For this reason, the square of differences is used.

The department is now part of a local area network which includes the departmental VAXstations. An IBM-compatible PC-XT has been installed in Manitoba II and this computer has been connected, through a modified parallel printer card, to the Nicolet signal averager (see figure 3-5 for schematic of card). This card and the accompanying software (see Appendix A) are capable of writing spectra from the signal averager directly to the fixed-disk of the PC-XT. This data may then be downloaded through an Ethernet card, via the local area network, directly to the VAXstations.

The effect is that data can now be downloaded from the signal averager to the PC in about 3 seconds. Further, the data can be transmitted to the VAXstation in about 30 seconds.

Once the data have been transferred to the Vaxstation, the analysis is carried out. The method of analysis has been improved over the course of this work. As described above, and by Ellis [El83] and Sidky [Si90], the previous method of computer-assisted analysis involved a least-squares fit of a quadratic curve to what were essentially chi-squared curves

of the unswitched peak in quadrant 0 and the peaks in quadrants 1,2 or 3. This fit was made over a given number of channels in the chi-squared data, but the number of channels chosen was somewhat arbitrary. Worse, it was observed that if a poor value for this number of channels was selected it could lead preferentially either to fitting the sides of the chi-squared curve rather than the area near the base (meaning that the technique might miss the actual base by some channels resulting in a substantial offset in ΔV and, hence, a substantial offset in the value of ΔM) or to having the parabola calculated during the quadratic fit be inverted (leading to a result for ΔM in which we can have no confidence) [Si90] (see figure 3-6).

In this work, the number of points for fitting the quadratic was chosen in order to minimize the chi-squared value of the fitted quadratic curve to the points. More points are used where the data most closely approximates a quadratic, fewer where the data give a poor approximation. This optimal number of points varies from run to run, but it is always chosen to minimize the chi-squared value of the fit.

In order to facilitate this fitting process, the points in the chi-squared spectra are always smoothed. In the past, this has entailed repeated application of a nine-point binomial algorithm, essentially a weighted average for four points on either side of the point of interest. Unfortunately, a smoothing algorithm of this type "smears" the data, taking a sharp peak and broadening it. The nine-point binomial algorithm does, however, lessen the effects of statistical noise.

The new level of computing power available to us allows the use of a superior technique. If we think of the peak we are interested in as extending over most of the channels in a quadrant, we find that statistical noise is basically high frequency in nature, while the features of the actual peak are rather low frequency. This allows us to transform the data in the quadrant from counts versus channels to counts versus frequency by applying a fast Fourier

transform. We then apply a low-pass filter to remove noise followed by an inverse transform which returns the smoothed data. In practice, the technique is slightly more involved; a constant level must be removed before the smoothing process begins. The actual code used to accomplish this task is the SMOOFT routine from the excellent "Numerical Recipes" collection [Pr86]. The SMOOFT routine, as used in the analysis program SPEAK, is included in Appendix B.

An example of the abilities of the SMOOFT routine are shown in figures 3-7 to 3-10. Figure 3-7 shows a mass spectral peak, as accumulated during the peak matching process. Figure 3-8 is the DC stripped and Fourier transformed version of figure 3-7. Figure 3-9 is the Fourier transformed data with the low-pass filter applied. Finally, figure 3-10 shows the fully reconstructed mass spectral peak, with noise removed.

These two improvements in the data acquisition and analysis system, coupled to greater attention to some technical details in the circuit by which ΔV is produced and measured (such as more frequent cleaning of contacts in voltage dividers), have resulted in significantly higher precision. Previously, 20 or more computer runs were needed to achieve final precision of 2-3 parts in 10^9. Now, the same precision can be achieved in only 4-8 computer runs. This improved error value per run corresponds, in rare cases, to the error approaching the theoretically determinable limit according to peak shape and number of counts.

In order to prove that the new data acquisition and analysis system does not introduce any systematic effects it was tested by matching a peak to itself. This should result in a mass difference of zero, within experimental error. The final mass difference value given by the test was 0.06(24) μu. This indicated that there were no systematic errors introduced by the Fourier-transform based smoothing technique or by the new method for selecting the

number of points for the quadratic fit. Moreover, it has been demonstrated that this new technique preserves the error associated with a given measurement, as limited by the number of counts in the peak and by the peak shape.

Figure 3.4 Computer Matching Timing

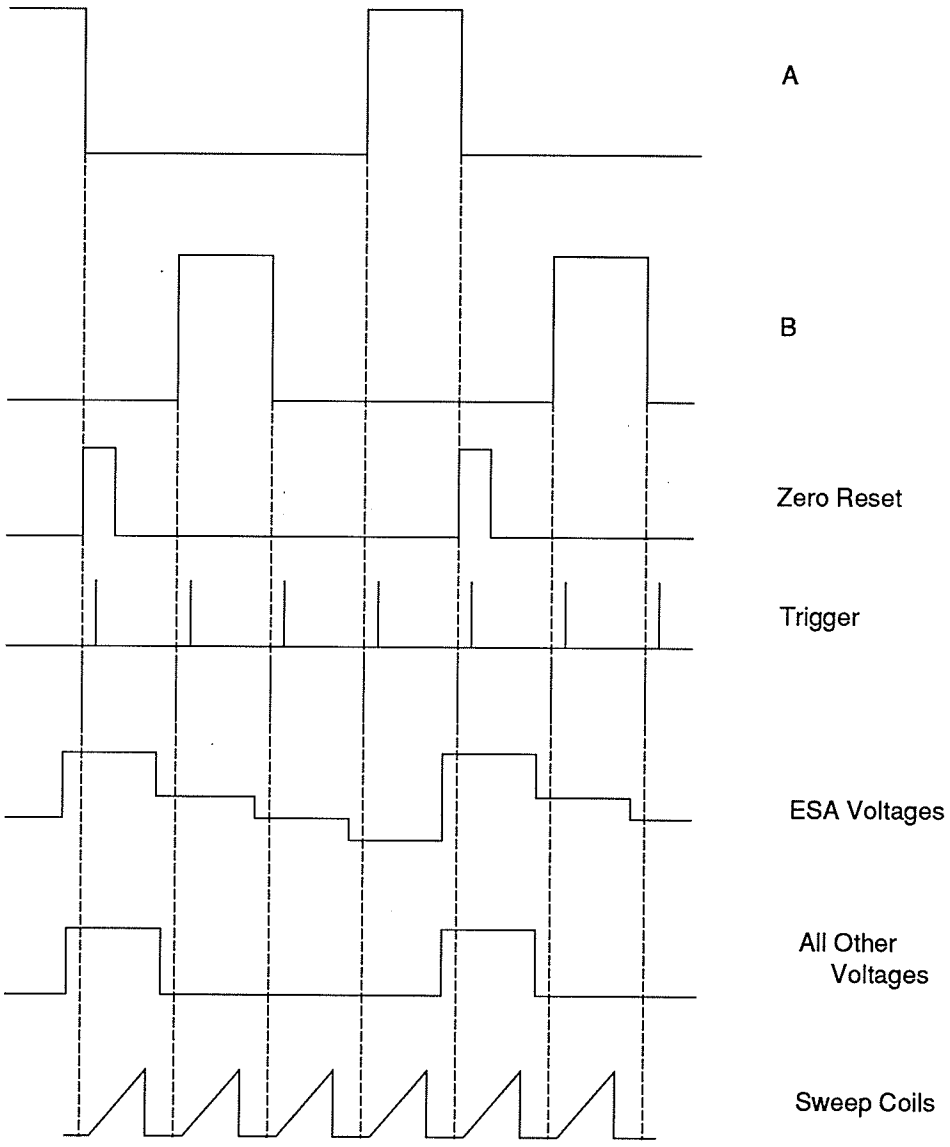

Figure 3.5 Data Acquisition Card Schematic

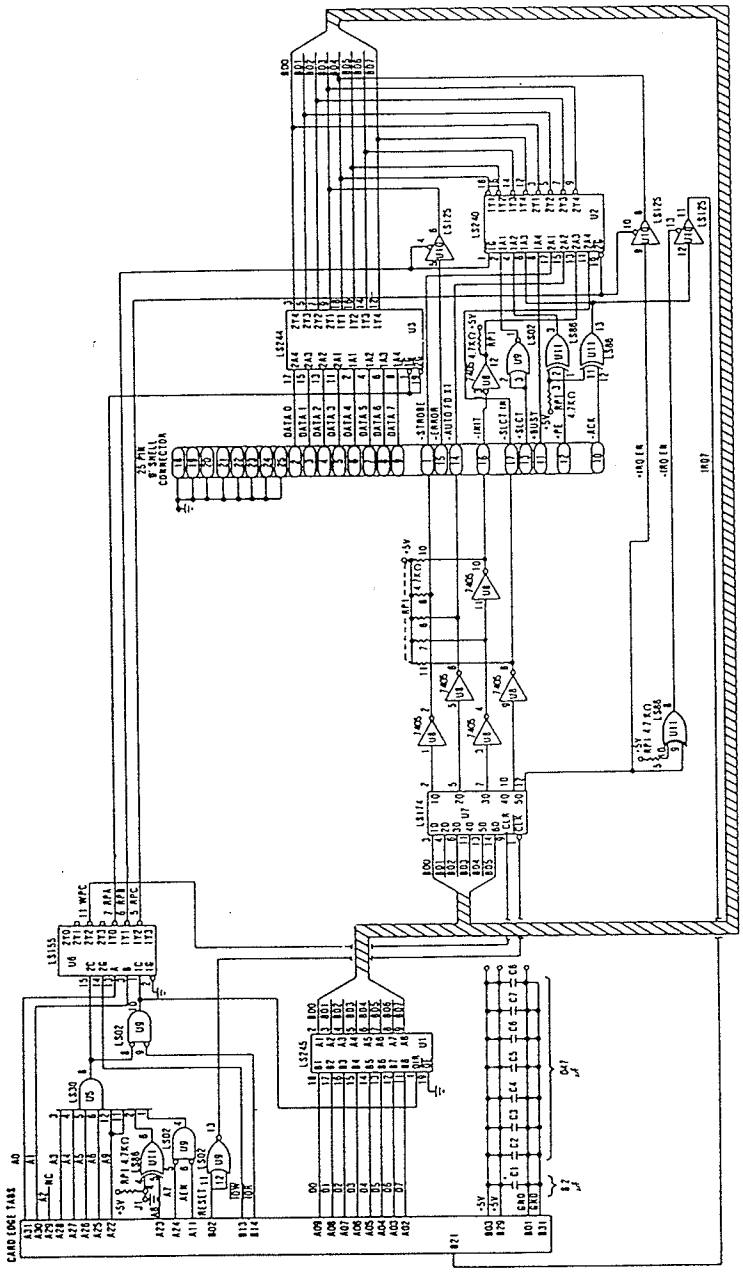

Figure 3.6 Chi-Squared Curve Fitting

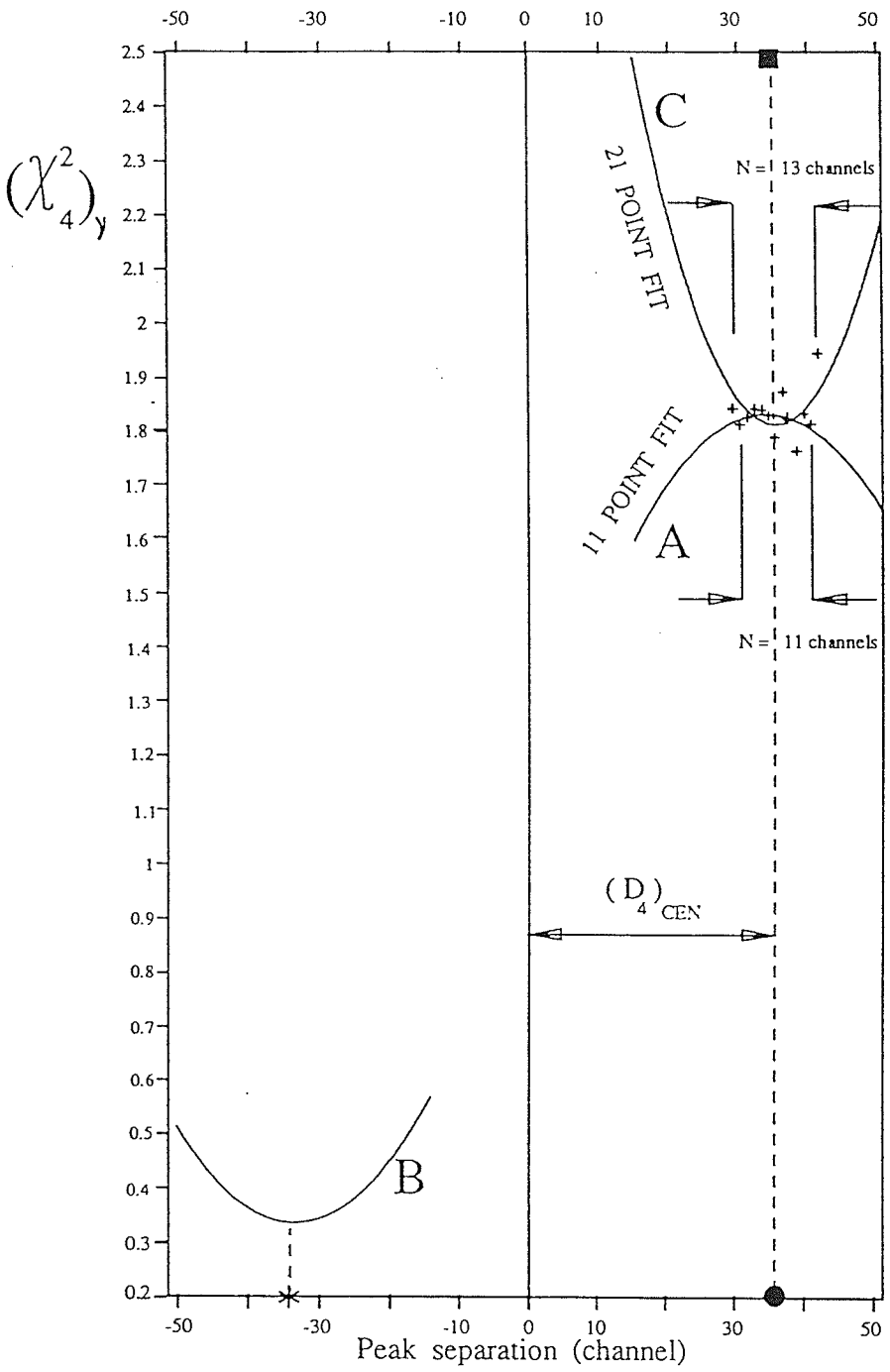

Figure 3.7 Raw Mass Spectral Data

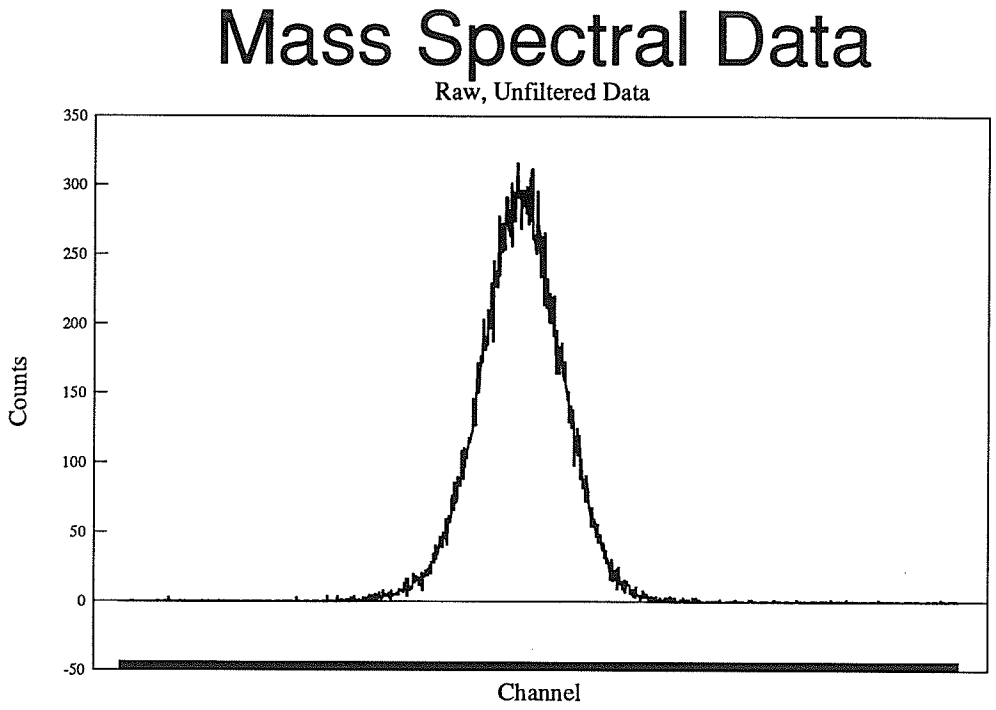

Figure 3.8 Unfiltered Fourier-Transformed Data

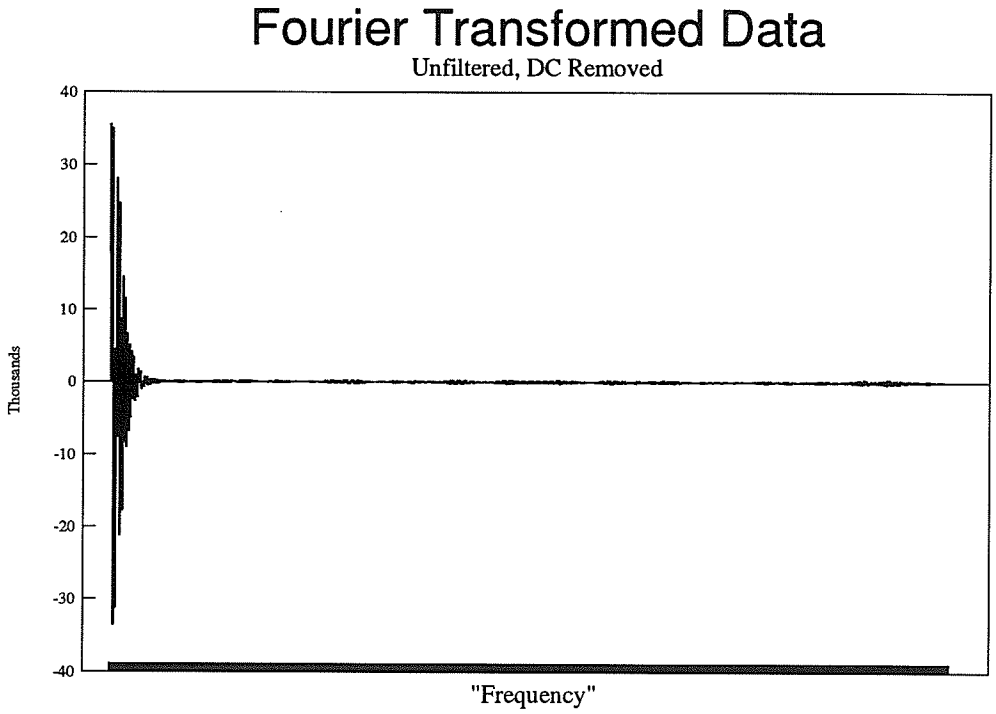

Figure 3.9 Filtered Fourier-Transformed Data

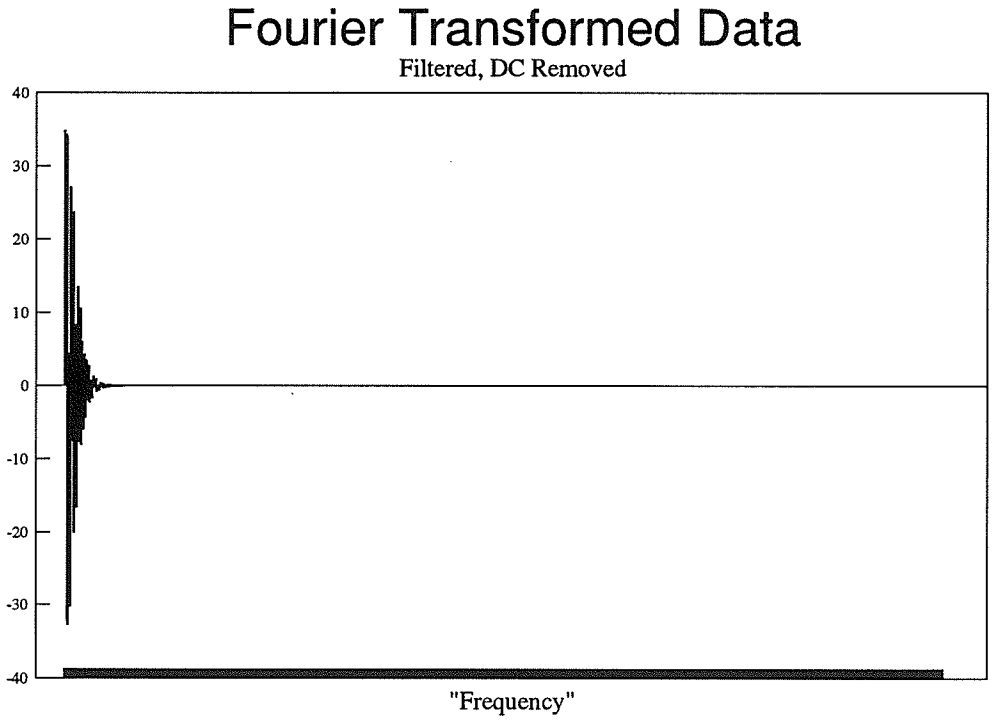

Figure 3.10 Smoothed Mass Spectral Data

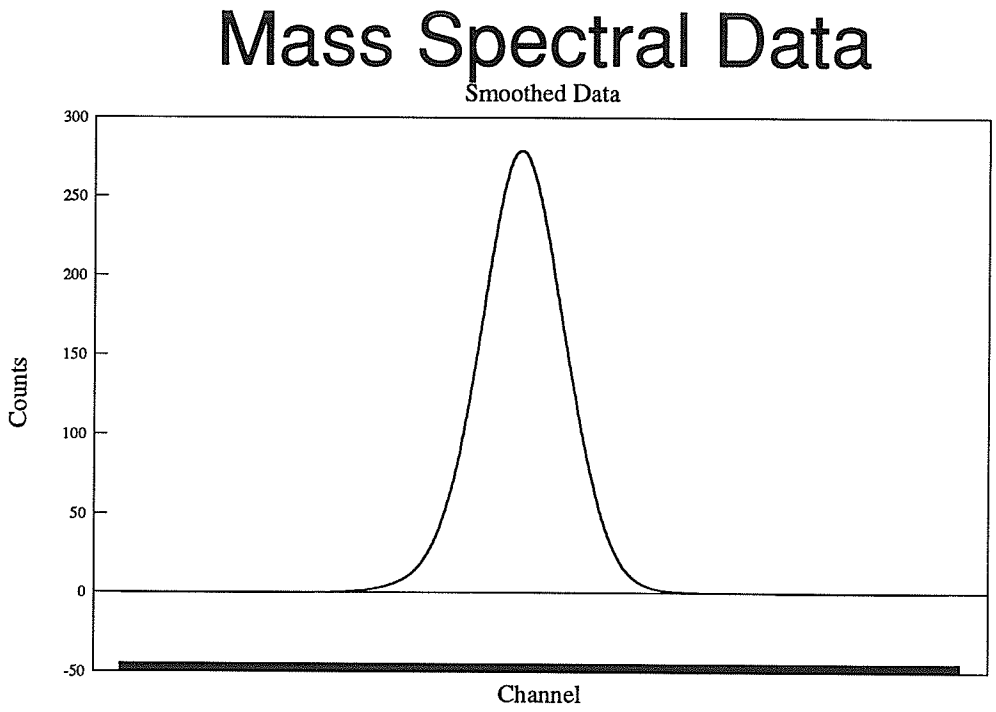

3.3 The ^{76}Ge-^{76}Se Experiment

3.3.1 Motivation for Measurement of the ^{76}Ge-^{76}Se Difference

As discussed in the previous chapters, the ^{76}Ge-^{76}Se difference provides important information regarding the existence of neutrinoless double-beta decay. If such a decay occurs, then there is strong evidence for a massive neutrino.

Various reports have been made on the progress of experiments searching for the neutrinoless decay mode of ^{76}Ge, both for the 0^+-0^+ transition to the ground state of ^{76}Se and the 0^+-2^+ transition to the first excited state of ^{76}Se [Av86, Av87, Bu90, Ca90, Va90]. The neutrinoless 0^+-0^+ Fermi transition will proceed if the electron neutrino is massive or if the weak force contains both right- and left-handed currents. The neutrinoless 0^+-2^+ Gamow-Teller transition will proceed only if the weak force is composed of an admixture of left- and right-handed currents.

All such experiments involve observing a sample of very pure germanium and summing the energies of decay products from all events in the crystal, including the pairs of electrons emitted during a double-beta decay. The spectrum of these summed energies is collected for extended periods of time. If the double-beta decay causing a pair of electrons to be emitted also produces a pair of anti-neutrinos, the anti-neutrinos will carry away a portion of the energy available from the decay when they escape the detector owing to their small cross-section of interaction with matter. Thus two-neutrino double-beta decay will result in a sum-energy spectrum which is a continuum [El87].

In neutrinoless double-beta, all of the energy of the decay is given to the beta particles; hence, the energy spectrum of these particles will show a sharp peak at the Q-value for the decay. This should be readily visible and easily interpreted. It is required, however, that the energy at which this peak occurs be known.

Through Einstein's mass-energy relation [Ei05], the Q-value for the decay may be determined by measuring the mass difference ^{76}Ge-^{76}Se.

In 1985, Ellis *et al.* [El85] used Manitoba II to measure 11 doublets in the area of the ^{76}Ge-^{76}Se region of the mass spectrum. These data over-determined the energy available for the double-beta decay of ^{76}Ge. The value found in the work of Ellis *et al.* was 2040.71(52) keV.

However, new precise data available from (n,γ) reactions by Hubert *et al.* [Hu89] are not in agreement with some of the mass differences measured by Ellis *et al.* Further, since internal consistency tests showed the work of Ellis *et al.* to be self-consistent, questioning even one of the difference measurements can call into question the entire series.

The Q-value of Ellis *et al.* indicated a region in the existing germanium double-beta decay spectra which gave no evidence for a neutrinoless double-beta decay mode. However, Avignone *et al.* [Av85] noted the presence of a statistically significant peak in the spectra of some of these experiments at a value about 4 keV above the Q-value measured by Ellis *et al.* If the Ellis value were incorrect through some unrecognized systematic error, and if this peak at 2045 keV were that of a zero-neutrino double-beta decay, it would imply either that the electron neutrino is massive or that right-handed weak currents exist.

The fundamental importance of the question of neutrino mass, coupled with concerns that the Q-value determined by Ellis *et al.* might be suspect, led to a decision to remeasure the most relevant doublets which over-determine the ^{76}Ge-^{76}Se mass difference. Recent improvements to Manitoba II were expected to make the resulting Q-value more precise.

3.3.2 Experimental Details

The materials used as samples were $GeCl_4$ and $SeCl_4$. $SeCl_4$ is a hygroscopic yellow crystalline material which is extremely toxic and has a sublimation point of only 196°C. As

such, $SeCl_4$ is too volatile to place in an oven inside the ion source. Instead, the $SeCl_4$ was placed in a stainless steel tube outside the ion source but connected to the internal gas oven by a feedthrough (figure 3-2). The steel tube was first wrapped in fiberglass and then with a nichrome ribbon. The whole assembly was again wrapped in fiberglass cloth to retain heat, thereby preventing $SeCl_4$ vapour from solidifying on the inside of the gas feedthrough and blocking gas flow.

$GeCl_4$ is a clear liquid with a high vapour pressure and is very corrosive. It was placed in a glass bottle and connected to the stainless steel tube containing the $SeCl_4$ by polyflo tubing. The tubing did break down under the action of the $GeCl_4$ vapour and had to be replaced about every three weeks. The high vapour pressure of the $GeCl_4$ sample meant that a Vacuum Generators MD6 leak valve was required to limit pressure in the ion source. This valve allows very precise adjustment of the gas flow and is resistant to the damage done by the $GeCl_4$.

Once sufficient quantities of the samples were being admitted to the ion source, measurement could begin. Unfortunately, an obstacle was encountered. Dimer ions of the forms $Se_2Cl_2^{2+}$ or $Ge_2Cl_2^{2+}$, were found to be present and were known to be unresolved from peaks of interest in several cases. The measured value of these mass differences was found to be artificially shifted in magnitude. Further, the formation of these dimers was shown to be highly dependent upon source temperature, the prevalence of these dimers increasing with increasing source temperatures. Accordingly, power dissipation in the ion source was kept as low as possible by running at low filament currents and keeping associated voltages low. In this manner, dimer production was greatly reduced. The absence of such dimers was confirmed by searching the mass spectrum in the neighbourhood of the doublet peaks for a clear signature of ions corresponding to the suspected contaminant.

When doublets involving a single chemical compound (*ie.* $^{76}Ge^{35}Cl$-$^{74}Ge^{37}Cl$ or $^{78}Se^{35}Cl$-$^{76}Se^{37}Cl$) were studied, the other compound was excluded from the source. This was accomplished easily when $GeCl_4$ was to be eliminated by simply cutting off the gas flow from the $GeCl_4$ reservoir bottle. For $SeCl_4$ to be excluded, however, it was necessary to clean the source by sandblasting, since $SeCl_4$ can adhere to the inside of the source. If this cleaning were not done, $SeCl_4$ could be present within the source for weeks after the external oven containing the sample is physically removed.

These procedures were used to eliminate contaminant ions from the mass spectrum. Using these procedures, we no longer need be concerned, for example, about the $^{76}Ge^{35}Cl$-$^{74}Ge^{37}Cl$ doublet being contaminated by the $^{76}Se^{74}Se^{37}Cl^{35}Cl$ dimer. However, these procedures do not remove the possibility of the above doublet being contaminated by a Ge_2Cl_2 dimer. The same is true for a SeCl-SeCl doublet being contaminated by a Se_2Cl_2 dimer.

In order to determine whether the $^{76}Ge^{35}Cl$-$^{74}Ge^{37}Cl$ doublet is being contaminated with a Ge_2Cl_2 dimer we look for a dimer of the form $^{76}Ge^{74}Ge^{37}Cl^{35}Cl$ (see figure 3-11). This dimer should occur as a peak exactly halfway between the peaks of the two desired ions. Any data which contained such a dimer peak was rejected, since some of these dimers are impossible to resolve from the desired ion peaks. Further, we do not know the intensity ratio between these dimer contaminants and the desired ions; therefore, a correction for the effect of such a contaminant is not possible.

There were no such contaminants present in any of the data collected for susceptible doublets. This was achieved primarily by keeping the power dissipated in the ion source low. That contaminants were absent is also evident by the rapid convergence of the mass differences to their final values, and by the consistency of these values with each other and

with external data.

Contamination is also a problem with cross-doublets such as $^{78}Se^{35}Cl$-$^{76}Ge^{37}Cl$. In these cases, the positions of all expected ionic contaminants were calculated and runs were taken at a resolving power sufficiently high to remove all contamination. Again, these results converged rapidly and were highly consistent with all available data.

There is one doublet where the above procedure for the removal of the effects of contaminants was unsuccessful. This is the $^{76}Se^{35}Cl$-$^{74}Ge^{35}Cl$ measurement. In this case, $^{74}Se^{37}Cl$ is present and will artificially increase the measured difference between the two ions. The required resolving power to remove the effect of this contaminant ion is in excess of 350,000. This resolving power was not attainable by Manitoba II given the ion source beam currents and the required final intensity. Obtaining a value for this doublet was fairly important to the measurement series, so an attempt to correct for the effect of the contaminant was made. Eight runs were taken, 64 spectra in all. Each spectrum was then subjected to a process which removed the effect of the contaminant. This required knowledge of the mass difference between $^{74}Se^{37}Cl$ and $^{76}Se^{35}Cl$ which was taken from the 1986 Atomic Mass Evaluation [Wa88]. It was also necessary to know the relative abundances of the two, a value which was taken from the Chart of Nuclides [CN87] and assigned a 10% error. With these data, and some of the measured voltages and calculated peak positions, it is possible to calculate a final value for the mass difference of this doublet.

Note that similar precautions were taken by Ellis *et al.* in their work. Unfortunately, it was not appreciated at that time how sensitive dimer production is to filament current and electron bombardment voltage. Moreover, all measurements by Ellis *et al.* were completed using the visual technique discussed earlier. While the visual method is very effective, it does not allow one to adequately determine that the resolving power in a given run is suf-

ficient to disregard the presence of contaminants, nor is there a permanent record of the data which can be re-analyzed for signs of contamination by dimers or other ions. No attempt was made by Ellis *et al.* to measure the $^{76}Se^{35}Cl$-$^{74}Ge^{37}Cl$ difference, since the doublet was too obscured by the $^{74}Se^{37}Cl$ ionic contaminant.

If a contaminant goes unrecognized, the consequences are severe. A contaminant peak only $\frac{1}{40}$ the size of the principal peak which it is affecting, but too close to be resolved, can shift the mass measurement by as much as 6 μu in this region (depending on the resolving power at which the instrument is operated).

The extreme sensitivity of contaminant production to source conditions, coupled with the impossibility of an *a posteriori* examination of the data of Ellis *et al.* for such contamination, lead us to recommend replacement of the values of Ellis *et al.* with those of the present work.

Figure 3.11 Search for Dimer Contaminant

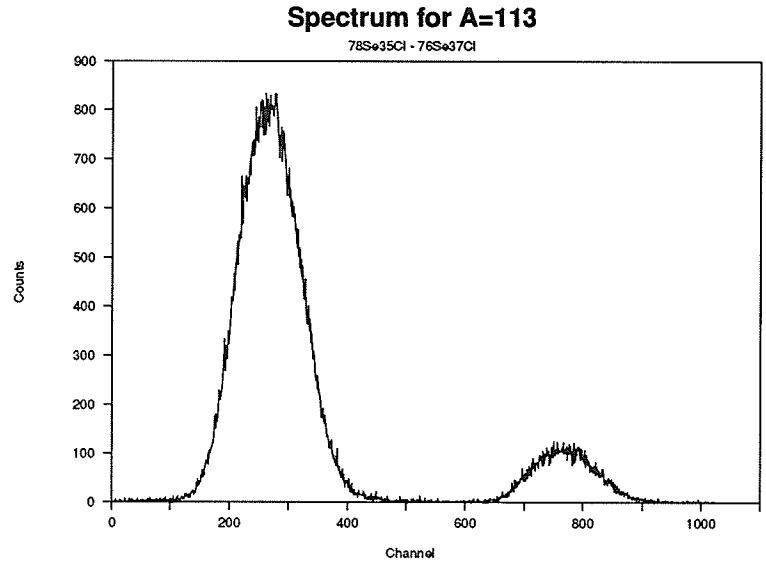

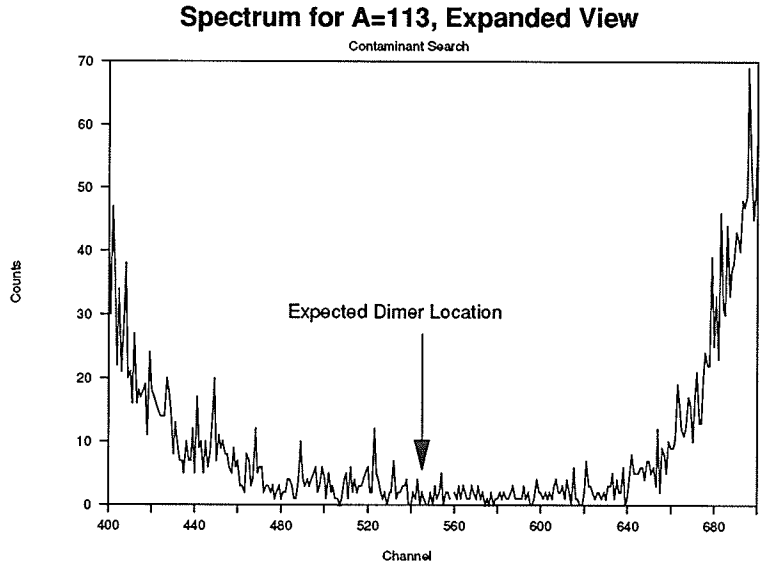

3.3.3 Results

There were six doublets measured during the course of this work, five of which directly overdetermine the desired ^{76}Ge-^{76}Se difference. See figure 3-12 for a schematic diagram of which isotopes were compared.

The five relevant differences were used as input data to a least-squares evaluation. The sixth measured doublet was not included in the least squares analysis, and was made only for comparison with new (n,γ) [Hu89] data in an attempt to assess a discrepancy between the previous measurement of Ellis *et al.* [El85] and other work. As well, a value for $^{78}Se^{35}Cl_2$-$^{74}Ge^{37}Cl_2$ was taken from the 1986 Atomic Mass Evaluation [Wa89] and placed into the least-squares program. The large error associated with this value (2.18 μu) serves to make it only a loose constraint to the least-squares evaluation.

The results of the least-squares analysis are:

Table 3-1

Code	Doublet	Input (μ*u*)	Output (μ*u*)	Chi-Sq
A	^{76}Ge-^{76}Se	2188.60 (42)	2188.48 (34)	0.08575
B	$^{76}Ge^{37}Cl$-$^{78}Se^{35}Cl$	1143.57 (72)	1143.82 (45)	0.11891
C	$^{78}Se^{35}Cl$-$^{76}Se^{37}Cl$	1044.58 (45)	1044.66 (39)	0.03061
D	$^{76}Se^{35}Cl$-$^{74}Ge^{37}Cl$	986.30 (65)	986.17 (42)	0.04019
E	$^{76}Ge^{35}Cl$-$^{74}Ge^{37}Cl$	3174.61 (41)	3174.65 (36)	0.00801
F	$^{74}Ge^{35}Cl$-$^{72}Ge^{37}Cl$	2052.01 (26)	-	-
g	$^{78}Se^{35}Cl_2$-$^{74}Ge^{37}Cl_2$	2030.40 (218)	2030.83 (57)	0.03862

The examination of loop closures of the raw data gives us insight into the internal consistency of these data. There are five available loops (see figure 3-12), all of which, when appropriately treated, should have a final sum/difference value of zero. Using the symbols for the doublets given in figure 3-12, we have:

$$A - B - C = 0.45 \pm 0.95$$

$$E - A - D = -0.30 \pm 0.88$$

$$g - C - D = -0.49 \pm 2.32$$

$$E - g - B = 0.64 \pm 2.33$$

$$g + A - E - C = -0.19 \pm 2.30$$

We may also compare the input values from this measurement series with those of Ellis *et al.* The results are:

Table 3-2

Doublet	This Work (μu)	Ellis *et al.* (μu)	Difference (μu)
^{76}Ge-^{76}Se	2188.60 (34)	2190.92 (59)	-2.32
$^{76}Ge^{37}Cl$-$^{78}Se^{35}Cl$	1143.57 (45)	1147.60 (92)	-4.03
$^{78}Se^{35}Cl$-$^{76}Se^{37}Cl$	1044.58 (39)	1042.03 (135)	+2.55
$^{76}Se^{35}Cl$-$^{74}Ge^{37}Cl$	986.30 (42)	-	-
$^{76}Ge^{35}Cl$-$^{74}Ge^{37}Cl$	3174.61 (36)	3170.41 (74)	+4.20
$^{74}Ge^{35}Cl$-$^{72}Ge^{37}Cl$	2052.01 (26)	2047.74 (71)	+4.27
$^{78}Se^{35}Cl_2$-$^{74}Ge^{37}Cl_2$	2030.40 (218)	-	-

One of the motivating factors in measuring this series was to resolve the discrepancy between the S_{2n} values derived from the mass differences measured by Ellis *et al.* and the S_{2n} values derived from the (n,γ) data of various groups. We are now in a position to compare all available data:

Table 3-3

Nuclide	S_{2n} (keV)			
	This Work	Ellis *et al.*	(n,γ)	Ref.
^{74}Ge	16979.22(26)	16983.21(61)	16978.5 (13)	Wa85, Hu89
^{78}Se	17917.56(37)	17919.50(79)	17916.7 (3)	En81, Yo85
^{76}Ge	15933.53(34)	15939.74(69)	15933.9 (10)	Wa85

Note that there is strong agreement between this work and recent (n,γ) data and poor agreement between this work and the values of Ellis *et al.*

Thus we have shown the new data presented in this work to be both internally and externally consistent. We now consider the implications of this new result for the ^{76}Ge-^{76}Se mass difference, 2188.48(34) μu or 2038.56(32) keV, when it is applied to the problem of detecting the neutrinoless double-beta decay of ^{76}Ge to ^{76}Se.

Figure 3.12 Schematic of Difference Measurements

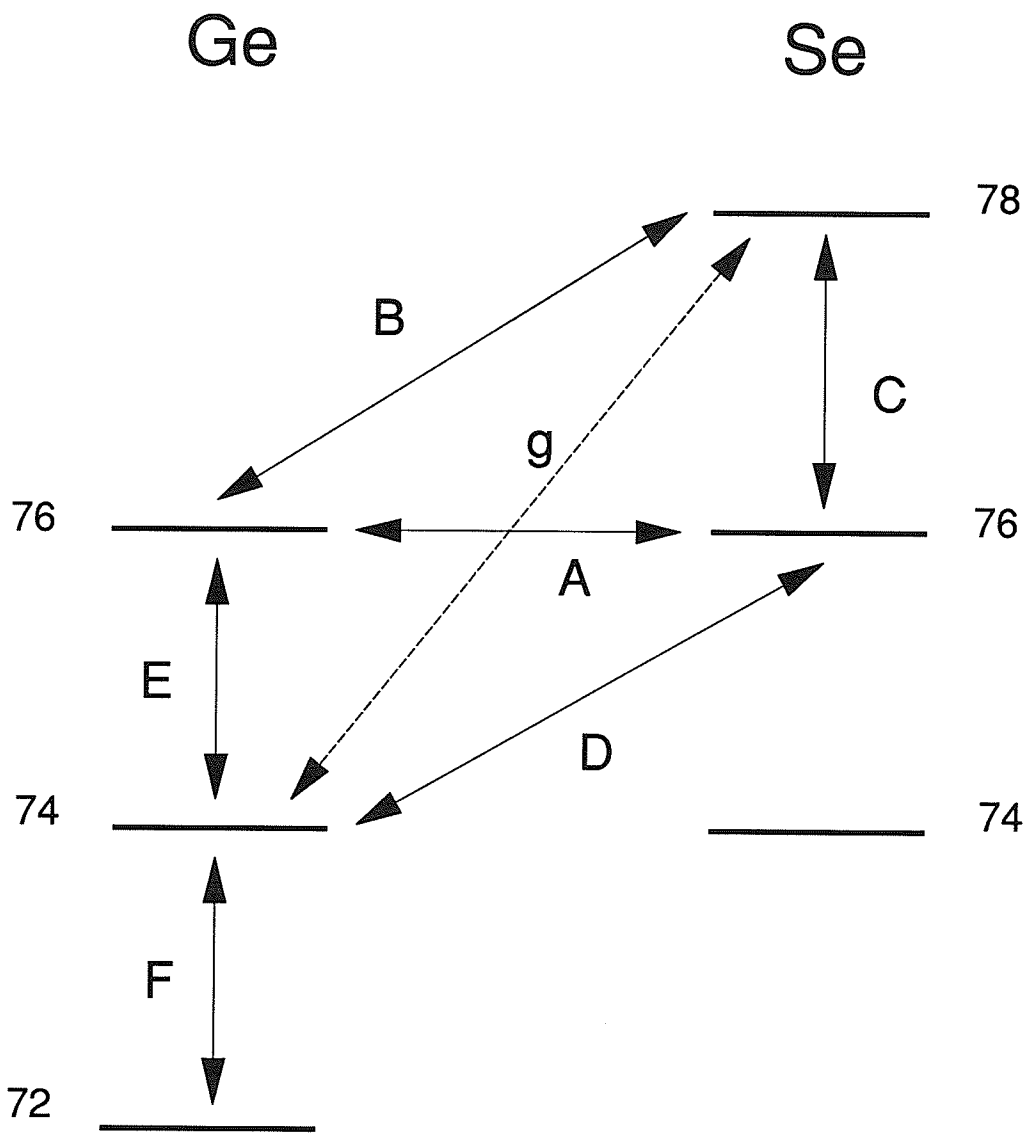

4 Implications of the Q-Value for ^{76}Ge-^{76}Se

4.1 New Data from Other Experiments on Neutrino Mass

Several reports concerning experiments searching for neutrinoless double-beta decay with hyperpure Ge metal detectors have appeared recently. In both 1986 and 1987, two separate reviews by Avignone *et al.* [Av86, Av87] discussed spectra of the lowest-background data collected by various experiments running at the times of these reviews. More recently, much improved spectra have been reported for Ge crystal detectors enriched in ^{76}Ge [Ca90, Va90].

These experiments all contain certain common factors. All are ultra-low background experiments in which all sources of background counts are greatly reduced. The result of this background reduction is a low count rate but a high confidence that events which are recorded have resulted from a decay in the sample. In addition, most of the experiments also utilize a veto shield surrounding the detector, composed of a scintillator which gives off a signal when a particle passes through it and then enters the Ge crystal. By excluding events in the Ge crystal which occur simultaneously with events in the veto shield, background is further reduced.

A variation on the above experiments, which is used primarily to search for the 0^+-2^+ neutrinoless double-beta decay of ^{76}Ge to ^{76}Se, is discussed below. These experiments also utilize a pure ^{76}Ge crystal detector, and typically also include a veto shield. Further, the apparatus incorporates an array of scintillator-type detectors inside the veto shield but external to the Ge crystal. By recording the energies of events in the Ge only when a gamma ray of 559 keV is detected by the scintillators in coincidence with the Ge event (559 keV being the de-excitation energy of the 2^+ state of ^{76}Se), it is possible to detect only the double-beta decays from the 0^+ state of ^{76}Ge to the 2^+ state of ^{76}Se.

Final results for both types of experiments are obtained in the same manner. The spectrum of decay product energies is examined for the presence of a characteristic peak at the Q-value of this decay. The half-life for the given decay mode can then be derived using a maximum likelihood analysis, since the number of such decays, sample size and counting time are known. The mass of the electron neutrino is then calculated on the basis of theory.

The Q-value given by Ellis *et al.* [El85] was used in a a search which did not reveal any evidence for $\beta\beta(0\nu)$ decay in the best decay-product spectra from ^{76}Ge samples [Av87, Ca90, Va90] (see figures 4-1, 4-2 and 4-3). A lower limit for the half-life of the zero-neutrino decay mode can be inferred from these spectra. The majorana neutrino mass is then derived from the limit on half-life and quoted as an upper limit. The smallest upper limit on the neutrino mass reported to date which utilizes the Ellis Q-value is that of Vasenko *et al.* [Va90], $\langle m_{\nu_e} \rangle < 1.4$eV.

One slightly discrepant result is that reported by Busto *et al.* [Bu90] for the collaboration working on the Frejus tunnel experiment. Here, a large Ge crystal is used to detect decays from the 0^+ ground state of ^{76}Ge to the 2^+ first excited state of ^{76}Se. This is done by requiring events in the Ge crystal to be coincident with a gamma event in surrounding NaI detectors. The gamma energy must be approximately that of the de-exciting gamma from the first excited state of the ^{76}Se, about 559 keV.

Busto *et al.* report two peaks in the region of their spectra corresponding to that indicated by the Q-value of Ellis *et al.* One peak in the Ge occurs at 1484 keV with an accompanying gamma ray at 561 keV. The other peak occurs at 1480 keV with a gamma at 606 keV. The first peak remains unidentified, but the peak at 1480 keV has been definitely linked to the presence of ^{214}Bi. A discussion of the implications of the new Q-value result in connection with this experiment will be presented in the next section.

Other types of experiments have also been used to investigate the neutrino mass question, regardless of its Majorana or Dirac character. Among these are several efforts concerned with examining the shape of the Kurie plot near the end-point of the electron energy spectrum for the decay of ^{3}H to ^{3}He. The latest of these efforts to report is that of Bowles *et al.* [Bo89] which provides a limit on the neutrino mass of $\langle m_{\nu_e} \rangle < 13.4$eV. Information on the shape of the Kurie curve is obscured by (a) statistical limitations and (b) the absence of information on the populations of possible final states for the ^{3}He atom. The available direct mass difference measurements, obtained by several groups using ion cyclotron resonance techniques, disagree with one another [St88].

The only supernova recorded using modern neutrino observatories, SN1987a, provided a unique opportunity to study the neutrinos produced in a supernova explosion. The raw data has been subjected to a mass analysis. A typical limit on the mass of the electron neutrino as a result of such analysis is $\langle m_{\nu_e} \rangle < 11$eV [Ba87].

As described in Chapters 2 and 3, mass difference measurements which were used to derive the Q-value for the double-beta decay of ^{76}Ge to ^{76}Se, as measured by Ellis *et al.*, disagree with those measured in this work. As stated in Chapter 3, we recommend that the values of Ellis *et al.* be replaced by the appropriate values from this work. Because the Q-value for the double-beta decay of ^{76}Ge to ^{76}Se has been altered by this work, a re-analysis of existing double-beta decay spectra is required.

4.2 New Result and Implications

The Q-value for the double-beta decay of ^{76}Ge to ^{76}Se is shown by this work to be 2038.56(32) keV. This value should be applied to the best decay-product energy spectra available for the ^{76}Ge crystal detectors in order to establish a half-life for the neutrinoless double-beta decay.

A maximum likelihood analysis was performed as described by Avignone *et al.* [Av87] on the spectrum given by Vasenko *et al.* [Va90]. This allows determination of a half-life for the 0^+-0^+ neutrinoless double-beta decay. This mode can proceed if the electron neutrino has a mass or if the weak current contains right-handed currents. The result of the analysis on the region of the spectrum surrounding 2039 keV is a most probable number of counts in the peak of -14.25 and a width for the likelihood function of 4.70. This allows the calculation of a limit on the half-life for the neutrinoless double-beta decay of ^{76}Ge to the ground state of ^{76}Se of:

$$T_{1/2}^{0\nu}(0^+ - 0^+) > 2.4 \times 10^{24} \text{years}(68\%\text{C.L.})$$

The background estimate for use in this analysis was $m = 3.58 \pm 0.28$ counts/keV. An inherent energy resolution for the Ge detector of $\sigma_x = 2.0$keV was used. All counts, other than those in a 7 keV region surrounding the channel corresponding to the new Q-value, are assumed to be background. A limit on the half-life for the neutrinoless double-beta decay is calculated by setting the value of c in the expression:

$$T_{1/2} = \frac{(\ln 2)Nt}{c}$$

equal to the width of the likelihood function. This yields a limit on the half-life to the 68% confidence interval.

It should be noted that some of the counts which might occur at 2039 keV due to neutrinoless double-beta decay could be attributed to the 0^+-2^+ form of this decay mode, where the de-excitation gamma ray from the 2^+ state of ^{76}Se has been completely absorbed in the Ge detector. However, a Monte Carlo analysis by Avignone *et al.* [Av85] has shown that there is a probability of 0.49, in his detector, that the gamma ray will completely escape. Thus, the level of such contamination of the 0^+-0^+ data by counts from the 0^+-2^+ decay is expected to be small, but the possibility should be noted.

One should also note that the entire analysis assumes that the counts in all channels not within 3 keV of the channel corresponding to 2039 keV are pure background and are not caused by contaminants.

The spectrum of Caldwell *et al.* [Ca90] also has no statistically significant number of events in the region of the channel corresponding to the Q-value of 2039 keV. The maximum likelihood technique gives a most probable number of counts of -63.4 with a width for the likelihood function of 10.6. The background value used was $m = 19.8 \pm 0.5$ and the energy resolution used was $\sigma_x = 1.64$keV. In this case, the limit on the half-life is:

$$T_{1/2}^{0\nu}(0^+ - 0^+) > 8.8 \times 10^{23} \text{years(68\%C.L.)}$$

A similar analysis may also be done for spectra from experiments searching for the neutrinoless double-beta decay from the ground state of ^{76}Ge to the first excited state of ^{76}Se, a 0^+-2^+ transition. This mode can occur only if the weak force has a right-handed component

in the current. Avignone *et al.* [Av86] give the spectrum from the PNL/USC detector for the region 559 keV below the 2039 keV area (figure 4-2). Once again, a maximum likelihood analysis was performed on the appropriate channels. This procedure yielded a half-life for this mode of:

$$T_{1/2}^{0\nu}(0^+ - 2^+) = (7.1^{+3.5}_{-3.4}) \times 10^{20} \text{years}(68\%\text{C.L.})$$

The background value was $m = 2.0 \pm 0.5$ counts/keV and the energy resolution of the detector was taken to be $\sigma_x = 1.64$.

This result is not conclusive, however. It is expected from theoretical considerations that the double-beta decay of ^{76}Ge to the first excited state of ^{76}Se would proceed at a slower rate than the decay to the ground state of ^{76}Se. Further, this result for the decay is much shorter than would be predicted theoretically. There is evidence from geochemical data that the two-neutrino mode of double-beta decay should have a much shorter half-life than either neutrinoless mode. A preliminary result by Miley *et al.* [Mi90] for the two-neutrino decay mode of ^{76}Ge is $(1.1^{+0.6}_{-0.3}) \times 10^{21}$ years (95% C.L.). It is possible that the work of Busto *et al.* may bear directly on this result.

Busto *et al.* [Bu90] have found that their spectrum searching for the 0^+-2^+ neutrinoless double-beta decay of ^{76}Ge is contaminated by counts at 1480 keV related to the presence of ^{214}Bi. This is precisely the energy at which our new results would place the decay of ^{76}Ge to the first excited state of ^{76}Se. Hence, we must conclude that, given the reported background levels of the Frejus experiment in 1990, this group would be unable to observe and to draw conclusions regarding the 0^+-2^+ neutrinoless double-beta decay of ^{76}Ge.

Since the effect of such contamination on an experiment searching for this mode of

neutrinoless double-beta decay in ^{76}Ge has not been considered, it appears that no conclusions should be drawn from the positive result of the maximum likelihood calculation on the data of Avignone *et al.*

We now consider the question of a Majorana mass for the electron neutrino. In any determination of the mass of the electron neutrino from the half-life for the neutrinoless double-beta decay, we must use expressions derived from involved nuclear structure calculations. Most of these expressions for the mass include three basic terms, one involving the Majorana mass of the electron neutrino and two involving right-handed coupling terms. Masses are generally determined as limits from the theoretical expressions by ignoring the right-handed couplings.

The theoretical expressions are of the form:

$$\langle m_{\nu_e} \rangle \leq \left\{ \frac{m_e^2 (T_{1/2}^{0\nu})^{-1}}{C_{mm}^{(0\nu)}} \right\}^{\frac{1}{2}} \text{eV}$$

The values of $C_{mm}^{(0)}$ are taken from the work of Tomoda and Faessler [To87], and from Muto, Bender and Klapdor [Mu89]. The limits on the electron neutrino Majorana mass are listed in table 4-1 (all limits are to the 68% confidence interval).

Table 4-1

	Tomoda, Faessler	Muto, Bender, Klapdor
Caldwell *et al.*	1.57 eV	1.63 eV
Vasenko *et al.*	0.95 eV	0.99 eV

The limits on the mass of the electron neutrino derived from data for the neutrinoless double-beta decay of ^{76}Ge are in agreement with the best limit from ^{3}H beta decay, $\langle m_{\nu_e} \rangle < 13.4$eV [Bo89]. The new results are also consistent with the limit from geochemistry, $\langle m_{\nu_e} \rangle < 0.44$eV [Ki83], and with the limits derived from the data of SN1987a, $\langle m_{\nu_e} \rangle < 11$eV [Ba87] and $\langle m_{\nu_e} \rangle < 20$eV [Ko87].

Data from the new generation of hyperpure ultralow background Ge detectors are leading to a sharp reduction in the upper limit on the electron neutrino mass, relative to the limits established by the first generation instruments. The new Q-value from this work is more precise and is more accurate than earlier measurements. Thus, the new Q-value will assist in further work directed at establishing improved limits on the mass of the electron neutrino, and thereby imposing constraints on the theory of fundamental particles.

Figure 4.1 Spectrum from ITEP/YePI Enriched Detector (1990)

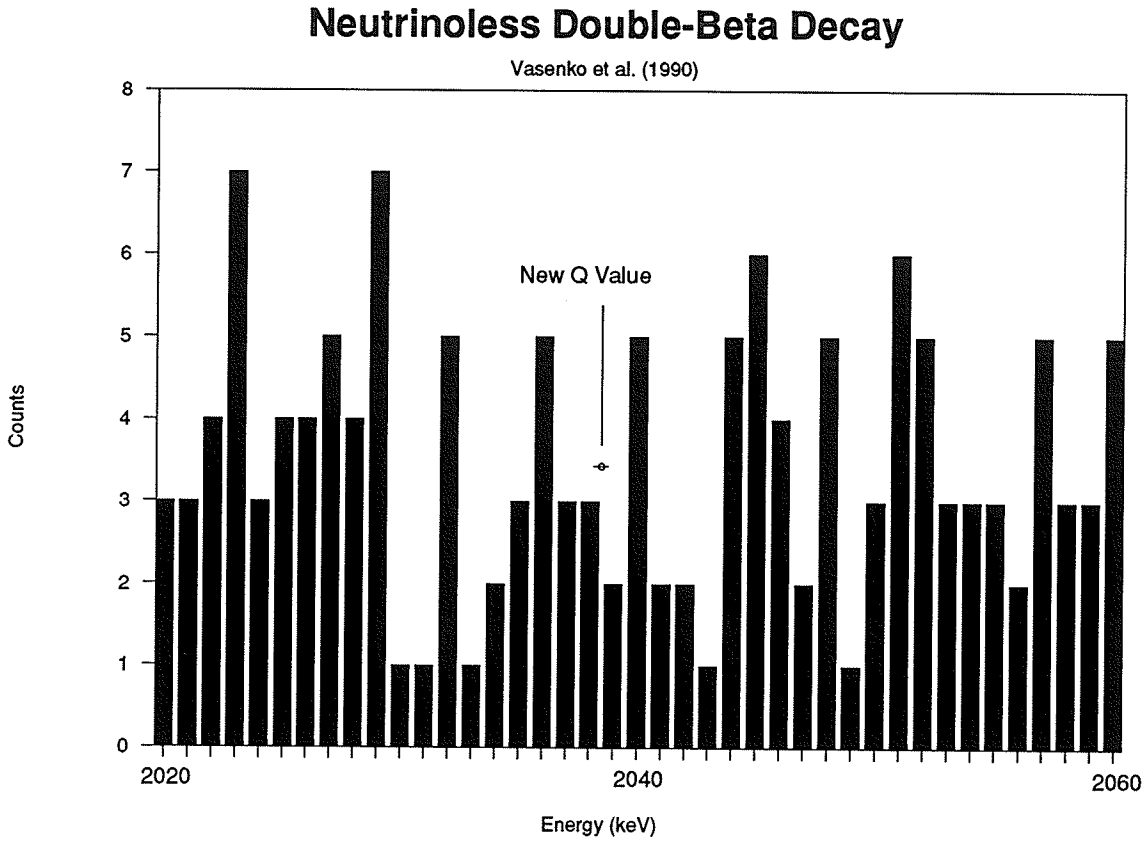

Figure 4.2 Spectrum from UCSB/LBL Detector (1990)

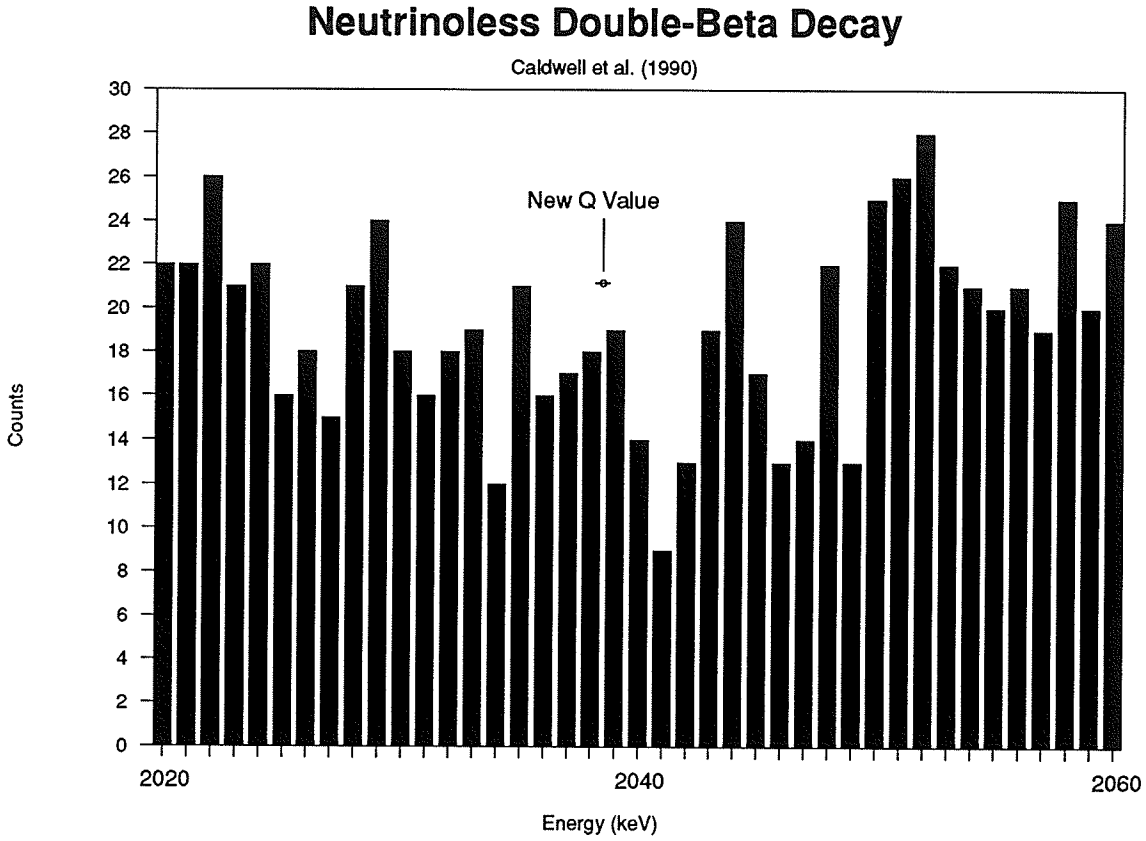

Figure 4.3 Spectrum from PNL/USC for 0^+-2^+ Neutrinoless Double-Beta Decay of ^{76}Ge

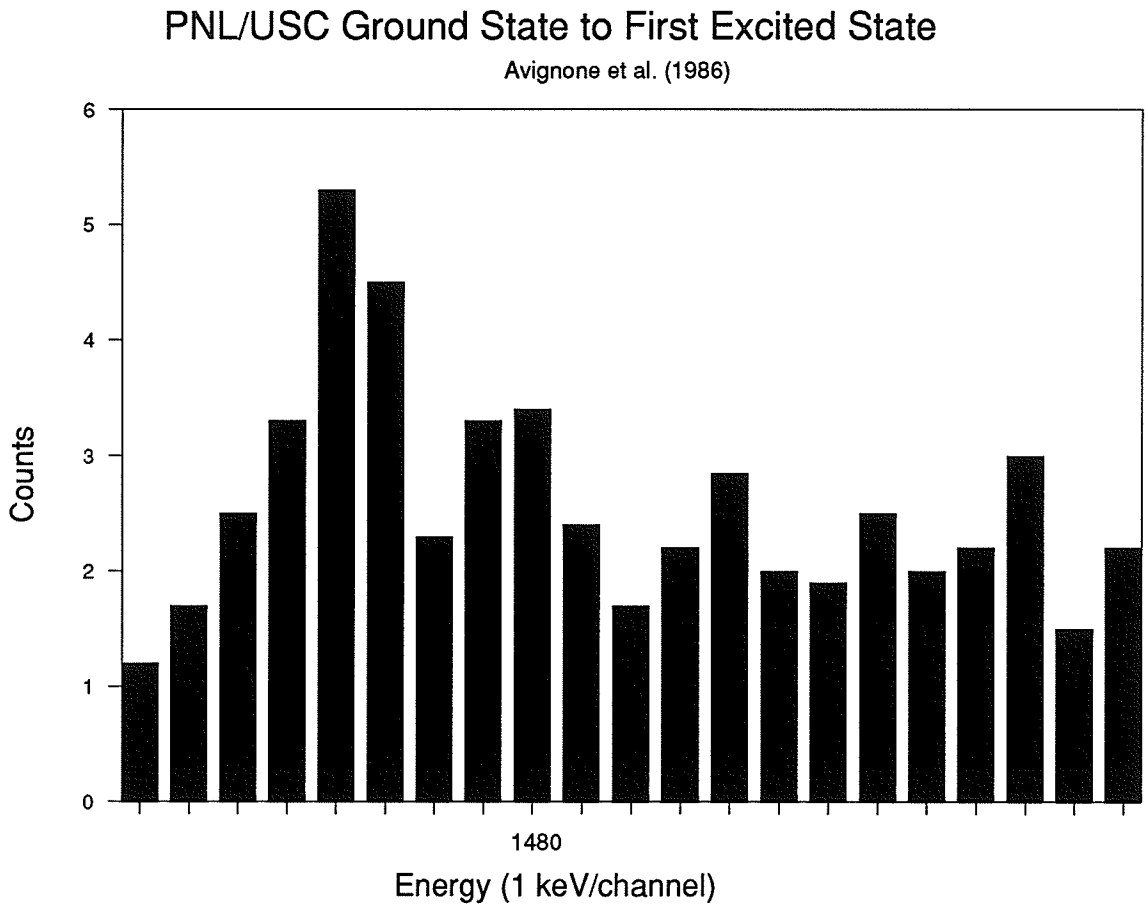

5 References

[As19] F.W. Aston (1912). *Philisophical Magazine*, **38**, 709.

[As23] F.W. Aston (1923). *Philisophical Magazine*, **45**, 934.

[Av85] F.T. Avignone III, R.L. Brodzinski, D.P. Brown, J.C. Evans Jr., W.K. Hensley, J.H. Reeves and N.A. Wogman (1985). *Physics Review Letters*, **54**, 2309.

[Av86] F.T. Avignone III, R.L. Brodzinski, J.C. Evans Jr., W.K. Hensley, H.S. Miley and J.H. Reeves (1986). *Physical Review C*, **34**, 2.

[Av87] F.T. Avignone III, H.S. Miley, R.L. Brodzinski and J.H. Reeves (1987). *Physical Review D*, **35**, No. 5, 1713.

[Ba33] K.T. Bainbridge (1933). *Physical Review*, **44**, 123.

[Ba36] K.T. Bainbridge and E.B. Jordan (1936). *Physical Review*, **50**, 282.

[Ba60] K.T. Bainbridge and P.E. Moreland (1960). **Proceedings of the International Conference on Nuclidic Masses**, ed. H.E. Duckworth. Toronto: University of Toronto Press.

[Ba67] R.C. Barber, J.O. Meredith, R.L. Bishop, H.E. Duckworth, M.E. Kettner and P. van Rookhuyzen (1967). **Proceedings of the Third International Conference on Atomic Masses**, ed. R.C. Barber, p717. Winnipeg: University of Manitoba Press.

[Ba71] R.C. Barber, R.L. Bishop, H.E. Duckworth, J.O. Meredith, F.C.G. Southon, P. van Rookhuyzen and P. Williams (1971). *Review of Scientific Instruments*, **42**, 1.

[Ba87] J.N. Bahcall and S.L. Glashow (1987). *Nature*, **326**, 462.

[Be66] J.L. Benson and W.H. Johnson (1966). *Physical Review*, **141**, 1112.

[Bi69] R.L. Bishop (1971). **Ph.D. Thesis**. Winnipeg: University of Manitoba Press.

[Bl36] W. Bleakney (1936). *American Physics Teacher*, **4**, 12.

[Bo87] S. Boris, A. Golutvin, L. Laptin, V. Lubimov, V. Nagovizin, V. Nozik, E. Novikov,

V. Soloshenko, I. Tihomirov, E. Tretjakov and N. Myasoedov (1987). *Physical Review Letters*, **58**, No. 20, 2019.

[Bo89] T.J. Bowles, J.L. Friar, R.G.H. Robertson, G.J. Stevenson, D.L. Wark, J.F. Wilkerson and D.A. Knapp (1989). **Proceedings of the Yamada Conference**. World Scientific Publishing Co. Pte. Ltd.

[Bu90] J. Busto, D. Dassie, O. Helene, Ph. Hubert, P. Larrieu, F. Leccia, P. Mennrath, M.M. Aleonard and J. Chevallier (1990). *Nuclear Physics*, **A513**, 291.

[Ca90] D.O. Caldwell, R.M. Eisberg, F.S. Goulding, B. Magnusson, A.R. Smith and M.S. Witherell (1990). *Nuclear Physics B (Proc. Suppl.)*, **13**, 547.

[CN77] F.W. Walker, G.J. Kirouac and F.M. Rourke. **Chart of the Nuclides, Twelfth Edition**. Knolls Atomic Power Laboratory.

[Co25] J.L. Costa (1925). *Annales de Physique, Paris*, **4**, 425.

[Co88] R. Cowsik (1988). *Physical Review D*, **37**, No. 6, 1685.

[Co89] E.A. Cornell, R.M. Weisskoff, K.R. Boyce, R.W. Flanagan Jr., G.P. Lafyatis and D.E. Pritchard (1989). *Physical Review Letters*, **63**, No. 16, 1674.

[De18] A.J. Dempster (1918). *Physical Review*, **11**, 316.

[De20] A.J. Dempster (1920). *Science*, **52**, 559.

[De35] A.J. Dempster (1935). *Nature*, **135**, 542.

[Dy90] G.R. Dyck (1990). **Ph.D. Thesis**. Winnipeg: University of Manitoba Press.

[Ei05] A. Einstein (1905). *Annalen der Physik*, **18**, 639.

[El83] R.J. Ellis (1983). **Ph.D. Thesis**. Winnipeg: University of Manitoba Press.

[El85] R.J. Ellis, R.C. Barber, G.R. Dyck, B.J. Hall, K.S. Sharma, C.A. Lander and H.E. Duckworth (1985). *Nuclear Physics*, **A435**.

[El87] S.R. Elliott, A.A. Hahn and M.K. Moe (1987). *Physical Review Letters*, **59**, No. 15,

1649.

[En81] G. Engler, R.E. Chrien, and I.H. Liou (1981). *Nuclear Physics*, **A372**, 125.

[Fe34] E. Fermi (1934). *Zeitschrift für Physik*, **88**, 161.

[Fi82] G.B. Field (1982). *Mercury*, **11**, No. 4, 74.

[Go86] E. Goldstein (1886). *Sitzungsberichte der Königlich Preussischen Academie der Wissenschaften zu Berlin*, **39**, 691.

[He34] R. Herzog (1934). *Zeitschrift für Physik*, **89**, 447.

[Hi59] H. Hintenberger and L.A. König (1959). **Advances in Mass Spectrometry, vol. 1**, ed. J.D. Waldrom, p16. London, New York, Paris: Pergamon Press.

[Hu89] Ph. Hubert (1989). Private communication.

[Ki83] T. Kirsten, H. Richter and E. Jessberger (1983). *Physical Review Letters*, **50**, 474.

[Ko79] K.S. Kozier, K.S. Sharma, R.C. Barber, J.W. Barnard, R.J. Ellis, V.P. Derenchuk and H.E. Duckworth (1979). *Canadian Journal of Physics*, **57**, 266.

[Ko87] E.W. Kolb, *et al.* (1987). *Physical Review D*, **35**, 3598.

[Ma34a] R. Herzog and J.H.E. Mattauch (1934). *Annalen der Physik, Leipzig*, **19**, 345.

[Ma34b] J. Mattauch and R. Herzog (1934). *Zeitschrift für Physik*, **89**, 786.

[Ma36] J.H.E. Mattauch (1936). *Physical Review*, **50**, 617.

[Ma37] E. Majorana (1937). *Nuovo Cimento*, **14**, 171.

[Ma76] H. Matsuda (1976). **Atomic Masses and Fundamental Constants, Vol. 5.**, p186. Ed. J.H. Sanders and A.H. Wapstra. New York, London: Plenum Press.

[Me71] J.O. Meredith (1971). **Ph.D. Thesis**. Winnipeg: University of Manitoba Press.

[Me72] J.O. Meredith, F.C.G. Southon, R.C. Barber, P. Williams and H.E. Duckworth (1972). *International Journal of Mass Spectrometry and Ion Physics*, **10**, 359.

[Mi90] H.S. Miley, F.T. Avignone III, R.L. Brodzinski, J.I. Collar and J.H. Reeves (1990).

Physical Review Letters, **65**, No. 25, 3092.

[Mu89] K. Muto, E. Bender and H.V. Klapdor (1989). *Z. Phys. A*, **334**, 187.

[Ni40] A.O. Nier (1940). *Review of Scientific Instruments*, **11**, 212.

[Pa33] W. Pauli (1933). *Handbuch der Physik, 24/1*. Berlin: Springer-Verlag.

[Pr86] W.H. Press, B.P. Flannery, S.A. Teukolsky and W.T. Vetterling (1986). **Numerical Recipes**, pp495-497. Cambridge, New York, Port Chester, Sydney, Melbourne: Cambridge University Press.

[Sc81] H. Schmeing, J.C. Hardy, E. Hagberg, W.L. Perry, J.S. Wills, J. Camplan and B. Rosenbaum (1981). *Nuclear Instruments and Methods*, **186**, 47.

[Si82] J. Silk (1982). *Nature*, **297**, 102.

[Si85] J.J. Simpson (1985). *Physical Review Letters*, **54**, No. 17, 1891.

[Si90] M.S. Sidky (1990). **Ph.D. Thesis**. Winnipeg: University of Manitoba Press.

[So73] F.C.G. Southon (1973). **Ph.D. Thesis**. Winnipeg: University of Manitoba Press.

[St89] S.T. Staggs, R.G.H. Robertson, D.L. Wark, P.P. Nguyen, J.F. Wilkerson and T.J. Bowles (1989). *Physical Review C*, **39**, No. 4, 1503.

[Sw31] W.F.G. Swann (1931). *Journal of the Franklin Institute*, **212**, 439.

[Th97] J.J. Thompson (1897). *Philosophical Magazine V*, **44**, 293.

[Th12] J.J. Thompson (1912). *Philosophical Magazine VI*, **24**, 209, 668.

[To87] T. Tomoda and A. Faessler (1987). *Phys. Lett. B*, **199**, No. 4, 475.

[Tu82] W. Tucker and K. Tucker (1982). *Mercury*, **11**, No. 4, 81.

[Va90] A.A. Vasenko, I.V. Kirpichnikov, V.A. Kuznetsov, A.S. Starostin, A.G. Djanyan, V.S. Pogosov, S.P. Shachysisyan and A.G. Tamanyan (1990). *Modern Physics Letters* **A5**, No. 17, 1299-1306.

[Wa85] A.H. Wapstra and G. Audi (1985). *The 1983 Atomic Mass Evaluation, Nuclear*

Physics, **A432**, 1.

[Wa88] A.H. Wapstra, G. Audi and R. Hoekstra (1988). *Atomic Data and Nuclear Data Tables*, **39**, No. 2, 281.

[Wi98] W. Wien (1898). *Verhandlungen der Physikalische Gesellschaft zu Berlin*, **17**, 1898.

[Wi02] W. Wien (1902). *Annalen der Physik und Chemie, Leipzig*, **8**, 224.

[Yo85] Y. Yokunaga, H. Seyfarth, R.A. Meyer, O.W. Schult, H.G. Borner, G. Barreau, H.R. Faust, K. Schreckenbach, S. Brant, V. Paar, M. Vouk and D. Vretenar (1985). *Nuclear Physics* **A439**, 427.

[Ze80] A. Zee (1980). *Physics Letters B*, **93**, 389.

6 Appendix A - Data Acquisition Program

```
      PROGRAM SPEC
C     Read spectrae from Fabritek Instrument (FTI) and store in a disk file.
C     Calls machine routines FTMEM, FTKEY, and FTGET in FTILIB.
C     13apr1988 - change function keys to 1-4,5-8 and display max counts.
      LOGICAL DUMP,GOON
      CHARACTER PROMPT*1
      INTEGER*2 TAG,C2
      DUMP = .FALSE.
      GOON = .FALSE.
      PROMPT = CHAR(1)
10    WRITE(*,20) PROMPT
20    FORMAT(' ',A1,' ',$)
      CALL FTKEY(C2)
      IF(C2.EQ.59*256)THEN
C F1 - Open new data file.
       CALL OPNNEW(TAG,DUMP)
       GOON = .TRUE.
      ELSE IF(C2.EQ.62*256)THEN
C F4 - Open old data file.
       CALL OPNOLD(TAG,DUMP)
       GOON = .TRUE.
      ELSE IF(C2.EQ.87*256)THEN
C SHIFT F4 - Continue interrupted file.
       CALL CONOLD(TAG,DUMP)
       GOON = .TRUE.
      ELSE IF(C2.EQ.66*256)THEN
C F6 - Exit.
       DUMP = .TRUE.
      ELSE
       CALL HELP1
      END IF
      IF(DUMP)GOTO 330
C Exit.
      IF(.NOT.GOON)GOTO 10
C     File is now open, on to data accumulation.
      PROMPT = CHAR(2)
30    WRITE(*,20) PROMPT
      CALL FTKEY(C2)
      IF(C2.EQ.63*256)THEN
C F5 - Read spectrum.
       CALL FRSPEC(TAG,DUMP)
      ELSE IF(C2.EQ.66*256)THEN
C F8 - Exit.
       CALL XIT(TAG,DUMP)
      ELSE IF(C2.EQ.84*256)THEN
C SHIFT F1 - Change TAG.
       CALL CHTAG(TAG)
      ELSE IF(C2.EQ.88*256)THEN
C SHIFT F5 - Backspace one spectrum.
       CALL BACKSP(TAG)
      ELSE IF(C2.EQ.91*256)THEN
C SHIFT F8 - Skip forward one spectrum.
       CALL SKIPFO(TAG)
      ELSE
       CALL HELP2
      END IF
      IF(.NOT.DUMP)GOTO 30
      CLOSE(1)
330   STOP 'End of SPECTRUM.'
      END
      SUBROUTINE OPNNEW(TAG,DUMP)
C     First check if there is room on the default disk for a set of ten
C     spectrae, 82000 bytes. If not, say another disk is needed and exit.
C     Set DUMP = .TRUE.. If there is room then ask for the name of the data
C     file. INQUIRE as to the file's existance. If it exists already, say
C     so and exit as before. If not, open a new file for use. Ask for
C     initial TAG (counter).
      LOGICAL DUMP,TOBE
      INTEGER*2 TAG,BPS,SPC,NFC
      INTEGER*4 MEM
```

```
      CHARACTER FLNAME*40
      DUMP = .FALSE.
      TAG = 1
      WRITE(*,*) 'Open New File.'
      CALL FTMEM(BPS,SPC,NFC)
      MEM = BPS*SPC*NFC
      IF(MEM.LT.82000)THEN
       WRITE(*,*) 'Less than 82000 bytes on the current'
       WRITE(*,*) 'disk. Not enough room for another set'
       WRITE(*,*) 'of ten spectrae.'
       WRITE(*,*) 'Try again with an empty, formatted disk.'
       DUMP = .TRUE.
      ELSE
      WRITE(*,10)
10    FORMAT(' Enter name for new data file: ')
      READ(*,20) FLNAME
20    FORMAT(A40)
      INQUIRE(FILE=FLNAME,EXIST=TOBE)
      IF(TOBE)THEN
       WRITE(*,*) 'A file with that name already exists on'
       WRITE(*,*) 'the current disk. Try a different name,'
       WRITE(*,*) 'or use F4 to append data onto the old'
       WRITE(*,*) 'file.'
       DUMP = .TRUE.
      ELSE
       OPEN(UNIT=1,FILE=FLNAME,STATUS='NEW')
       WRITE(*,40)
40    FORMAT(' Enter number for new TAG (1): ',$)
       READ(*,*) TAG
       IF(TAG.LT.1)THEN
        WRITE(*,*) 'TAG must be greater than zero. Set to 1.'
        TAG = 1
       ELSE IF(MOD(TAG,10).NE.1)THEN
        WRITE(*,*) 'MOD(TAG,10) not equal to 1.'
        TAG = 1 + (TAG+9)/10
        WRITE(*,*) 'TAG set to',TAG
       END IF
      END IF
      END IF
      RETURN
      END
      SUBROUTINE OPNOLD(TAG,DUMP)
C     Check for room on disk, exit if none.
C     Check existance of file, if not, warn and dump.
C     If exists, open and read to the end. If last tag not a multiple
C     of ten, warn, close, and dump.
C     If all ok, set tag to +1 of last, ready to append to file.
      LOGICAL DUMP,TOBE,ENF
      INTEGER*2 TAG,BPS,SPC,NFC,JSPEC(1024,4)
      INTEGER*4 MEM
      CHARACTER FLNAME*40
      DUMP = .FALSE.
      TAG = 1
      WRITE(*,*) 'Open Old File.'
      CALL FTMEM(BPS,SPC,NFC)
      MEM = BPS*SPC*NFC
      IF(MEM.LT.82000)THEN
       WRITE(*,*) 'Less than 82000 bytes free on current'
       WRITE(*,*) 'disk. Not enough room for another set'
       WRITE(*,*) 'of ten spectrae. Try again with an'
       WRITE(*,*) 'empty, formatted disk, using F1 to open'
       WRITE(*,*) 'a new data file.'
       DUMP = .TRUE.
      ELSE
      WRITE(*,10)
10    FORMAT(' Enter name of old data file: ')
      READ(*,20) FLNAME
20    FORMAT(A40)
      INQUIRE(FILE=FLNAME,EXIST=TOBE)
      IF(.NOT.TOBE)THEN
       WRITE(*,*) 'Given file does not exist on the current'
       WRITE(*,*) 'disk. Try another name or create a new'
       WRITE(*,*) 'file with F1.'
```

```
        DUMP =.TRUE.
       ELSE
        OPEN(UNIT=1,FILE=FLNAME,STATUS='OLD')
30      CALL RDFL(TAG,JSPEC,ENF)
        IF(.NOT.ENF) GOTO 30
        WRITE(*,*) 'Last TAG in file was',TAG
        IF(MOD(TAG,10).NE.0)THEN
         WRITE(*,*) 'Last TAG not a multiple of ten.'
         WRITE(*,*) 'Use SHIFT F4 to continue an interrupted'
         WRITE(*,*) 'set of ten spectrae.'
         DUMP = .TRUE.
         CLOSE(1)
        ELSE
         TAG = TAG + 1
         WRITE(*,*) 'TAG for next spectrum is',TAG
        END IF
       END IF
       END IF
       RETURN
       END
       SUBROUTINE CONOLD(TAG,DUMP)
C      Exit if file does not exist. Open, read to end. Last tag
C      probably not a multiple of 10. Set tag to last + 1, figure
C      space needed to complete. If not enough space, warn, close,
C      exit. If ok, ready to append to file. Display last and
C      current tag.
       LOGICAL DUMP,TOBE,ENF
       INTEGER*2 TAG,BPS,SPC,NFC,JSPEC(1024,4),J
       INTEGER*4 MEM,RMEM
       CHARACTER FLNAME*40
       DUMP = .FALSE.
       TAG = 1
       WRITE(*,*) 'Continue Old File.'
       WRITE(*,10)
10     FORMAT(' Enter name of interrupted data file: ')
       READ(*,20) FLNAME
20     FORMAT(A40)
       INQUIRE(FILE=FLNAME,EXIST=TOBE)
       IF(.NOT.TOBE)THEN
        WRITE(*,*) 'Given file does not exist on current'
        WRITE(*,*) 'disk. Try another name or create a new'
        WRITE(*,*) 'file with F1.'
        DUMP = .TRUE.
       ELSE
       OPEN(UNIT=1,FILE=FLNAME,STATUS='OLD')
30     CALL RDFL(TAG,JSPEC,ENF)
       IF(.NOT.ENF)GOTO 30
       WRITE(*,*) 'Last TAG in file was',TAG
       J = 10 - MOD(TAG,10)
       WRITE(*,*) J,' spectrae needed'
       WRITE(*,*) 'to complete this set.'
       CALL FTMEM(BPS,SPC,NFC)
       MEM = BPS*SPC*NFC
       IF(J.EQ.0)THEN
        IF(MEM.LT.82000)THEN
         WRITE(*,*) 'Less than 82000 bytes on current disk.'
         WRITE(*,*) 'Not enough room for another set of ten'
         WRITE(*,*) 'spectrae. Try again with an empty,'
         WRITE(*,*) 'formatted disk, using F1 to open a new'
         WRITE(*,*) 'data file.'
         DUMP = .TRUE.
        END IF
       ELSE
        RMEM = J*8200
        IF(MEM.LT.RMEM)THEN
         WRITE(*,*) 'Less than',RMEM,' bytes'
         WRITE(*,*) 'on current disk. Not enough room for'
         WRITE(*,*) 'the rest of this set of ten spectrae.'
         WRITE(*,*) 'You''ll have to copy the data file '
         WRITE(*,*) 'to a new disk with more room.'
         DUMP = .TRUE.
        END IF
       END IF
```

```
      IF(DUMP)THEN
       CLOSE(1)
      ELSE
       TAG = TAG + 1
       WRITE(*,*) 'TAG for the next spectrum is',TAG
      END IF
      END IF
      RETURN
      END
      SUBROUTINE HELP1
      WRITE(*,*) '----------First stage commands:'
      WRITE(*,*) '     F1: Create a new data file.'
      WRITE(*,*) '     F4: Open an old data file to add'
      WRITE(*,*) '         a new set of ten spectrae.'
      WRITE(*,*) 'SHIFT F4: Open an old data file to'
      WRITE(*,*) '         continue an interrupted set'
      WRITE(*,*) '         of ten spectrae.'
      WRITE(*,*) '     F8: Exit.'
      RETURN
      END
      SUBROUTINE HELP2
      WRITE(*,*) '----------Second stage commands:'
      WRITE(*,*) 'SHIFT F1: Change the TAG number.'
      WRITE(*,*) '     F5: Read a spectrum from the'
      WRITE(*,*) '         Fabritek Instrument.'
      WRITE(*,*) 'SHIFT F5: Backspace over the last'
      WRITE(*,*) '         spectrum.'
      WRITE(*,*) 'SHIFT F8: Skip to the next spectrum.'
      WRITE(*,*) '     F8: Exit.'
      RETURN
      END
      SUBROUTINE RDFL(TAG,JSPEC,ENF)
      LOGICAL ENF
      INTEGER*2 J,K,JSPEC(1024,4),TAG
      ENF = .FALSE.
      READ(1,10,END=100) TAG
10    FORMAT(A2)
      DO 20 J=1,4
       READ(1,30,END=100) (JSPEC(K,J),K=1,1024)
20    CONTINUE
30    FORMAT(1024A2)
      RETURN
100   ENF = .TRUE.
      BACKSPACE 1
      RETURN
      END
      SUBROUTINE FRSPEC(TAG,DUMP)
C     Assume there's enough space on the disk for this spectrum.
C     Read the spectrum. Check for wild points - give warning if
C     neccessary. Ask for <CR> to store in current file at current
C     position, other character to abort without incrementing TAG.
C     If ok, write TAG, spectrum. If TAG is zero mod ten, check
C     space for new set of ten. If no space, warn and dump.
C     If space, increment TAG.
      LOGICAL DUMP
      INTEGER*2 TAG,JSPEC(1024,4),C2,J,K,BPS,SPC,NFC
      INTEGER*4 MEM
      DUMP = .FALSE.
      DO 5 J=1,4
      DO 6 K=1,1024
       JSPEC(K,J) = 0
6     CONTINUE
5     CONTINUE
      WRITE(*,10) TAG
10    FORMAT(' Reading #',I4,'...',$)
      CALL FTIGET(JSPEC)
      WRITE(*,15)
15    FORMAT(' Got it. Max counts:')
      CALL WILD(JSPEC)
      WRITE(*,*) 'Hit ENTER to store spectrum, anything'
      WRITE(*,*) 'else to try again:'
      CALL FTKEY(C2)
      IF(C2.NE.13)THEN
```

```
        WRITE(*,*) 'Press F5 to read spectrum number',TAG
       ELSE
        WRITE(*,20) TAG
20     FORMAT(' Writing spectrum',I4,'...',$)
        WRITE(1,30) TAG
30     FORMAT(A2)
        DO 40 J=1,4
         WRITE(1,50) (JSPEC(K,J),K=1,1024)
40      CONTINUE
50     FORMAT(1024A2)
        WRITE(*,60)
60     FORMAT(' All done.')
        IF(MOD(TAG,10).EQ.0)THEN
         WRITE(*,*) 'Set of ten spectrae now complete.'
         CALL FTMEM(BPS,SPC,NFC)
         MEM = BPS*SPC*NFC
         IF(MEM.LT.82000)THEN
          WRITE(*,*) CHAR(7),CHAR(7)
          WRITE(*,*) 'No space on disk for another set of ten'
          WRITE(*,*) 'spectrae - start a new data file on a'
          WRITE(*,*) 'blank, formatted disk with command F1.'
          DUMP = .TRUE.
         END IF
        END IF
        TAG = TAG + 1
        WRITE(*,*) 'TAG for next spectrum is',TAG
       END IF
       RETURN
       END
       SUBROUTINE WILD(JSPEC)
C      Announce presence of wild points in spectrum.
C      Just write maximum counts for each quadrant.
       INTEGER*2 JSPEC(1024,4),J,K,M,WC,MAXC(4)
       WC = 0
       DO 100 J=1,4
        MAXC(J) = 0
        DO 50 K=3,1023
         IF(JSPEC(K,J).GT.MAXC(J))THEN
          MAXC(J) = JSPEC(K,J)
         END IF
50      CONTINUE
100    CONTINUE
       WRITE(*,200) MAXC
200    FORMAT(4I7)
       RETURN
       END
       SUBROUTINE XIT(TAG,DUMP)
       LOGICAL DUMP
       INTEGER*2 TAG,C2
       WRITE(*,*) 'Exit.'
       IF(MOD(TAG,10).EQ.1)THEN
        DUMP = .TRUE.
       ELSE
        WRITE(*,*) CHAR(7)
        WRITE(*,*) 'Set of ten spectrae is not complete.'
        WRITE(*,*) 'Hit X to confirm exit:'
        CALL FTKEY(C2)
        IF(C2.EQ.88.OR.C2.EQ.120)THEN
         WRITE(*,*) 'Exit confirmed.'
         DUMP = .TRUE.
        ELSE
         WRITE(*,*) 'Exit aborted, program continues.'
         DUMP = .FALSE.
        END IF
       END IF
       RETURN
       END
```

```
      SUBROUTINE CHTAG(TAG)
      INTEGER*2 TAG
      WRITE(*,*) 'Current tag value for next spectrum is',TAG
10    WRITE(*,20)
20    FORMAT('$Enter new value: ')
      READ(*,*,ERR=10) TAG
      RETURN
      END
      SUBROUTINE BACKSP(TAG)
      INTEGER*2 TAG,J,T
      WRITE(*,*) 'Backspace.'
      DO 10 J=1,5
       BACKSPACE 1
10    CONTINUE
      READ(1,20,END=100) T
20    FORMAT(A2)
      BACKSPACE 1
      WRITE(*,*) 'Old TAG was',TAG
      WRITE(*,*) 'Current TAG is',T
      TAG = T
      RETURN
100   WRITE(*,*) 'File is empty. TAG is still',TAG
      BACKSPACE 1
      RETURN
      END
      SUBROUTINE SKIPFO(TAG)
      INTEGER*2 TAG,JSPEC(1024,4),J,K,T1,T2
      WRITE(*,*) 'Skip.'
      READ(1,10,END=300) T1
10    FORMAT(A2)
      DO 20 J=1,4
       READ(1,30,END=300) (JSPEC(K,J),K=1,1024)
20    CONTINUE
30    FORMAT(1024A2)
      READ(1,10,END=400) T2
      BACKSPACE 1
      IF(TAG.NE.T1)THEN
       WRITE(*,*) CHAR(7)
       WRITE(*,*) 'Old internal tag not same as old tag'
       WRITE(*,*) 'in file, which was',T1
      END IF
      WRITE(*,*) 'Old TAG was',TAG
      TAG = T2
      WRITE(*,*) 'New TAG is',TAG
      RETURN
300   WRITE(*,*) 'At End of File. TAG still',TAG
      BACKSPACE 1
      RETURN
400   WRITE(*,*) 'At end of file. TAG was',TAG
      TAG = T1 + 1
      WRITE(*,*) 'Incremented to',TAG
      BACKSPACE 1
      RETURN
      END


; Subroutines to be called from FORTRAN to read spectrums from the
; Fabritek Intrument (FTI), and to do things to the 'printer' data
; and control ports at 278H and 27AH.
; Call with the form:
; INTEGER*2 JSPEC(0:4095),JDATA,JCONT,BPS,SPC,NFC,C2
; (or jspec(1,4096), OR JSPEC(1024,4) )
; CALL FTIGET(JSPEC)          ! Returns spectrum in array JSPEC.
; CALL FTIHI                  ! Sets the strobe line to +5V.
; CALL FTILO                  ! Sets the strobe line to 0V.
; CALL FTIPLS                 ! Makes a pulse on the strobe line - 0, then 5V.
; CALL FTIRDT(JDATA)          ! Returns the contents of the data port (0-255).
; CALL FTIRCN(JCONT)          ! Returns the contents of the control port.
;                             ! Strobe line is bit 0 (0-7).
; CALL FTMEM(BPS,SPC,NFC)! Returns BytesPerSector, SectorsPerCluster,
;         ! and NumberofFreeClusters for the default
;         ! disk drive.
```

```
; CALL FTKEY(C2)! Waits for keypress, echoes, and returns in C2.
;       ! Key in C2(HI), or NUL and extended in C2(LO).
; But first, a few handy macros:
INTO   MACRO            ; Shuffles base pointer, saves registers.
       PUSH   BP
       MOV    BP,SP
       PUSH   AX
       PUSH   BX
       PUSH   DX
       ENDM
OUTOF  MACRO            ; Pops registers from stack, unshuffles BP.
       POP    DX
       POP    BX
       POP    AX
       MOV    SP,BP
       POP    BP
       ENDM
MSIX   MACRORG; Shift register left by six - *64.
       SHLRG,1
       SHLRG,1
       SHLRG,1
       SHLRG,1
       SHLRG,1
       SHLRG,1
       ENDM
FPULSE MACRO            ; Output a pulse on the strobe line LO,HI.
       MOV    DX,CPORT
       MOV    AX,LOBIT
       OUT    DX,AL
       MOV    AX,HIBIT
       OUT    DX,AL
       ENDM
FRDBYT MACRO  BYTEN     ; Read one of the 3 bytes and stash it away.
       MOV    DX,DPORT
       IN     AL,DX
       MOV    BYTEN,AL
       ENDM

FREAD3 MACRO            ; Read all three bytes and store.
       FRDBYT BHI
       MOV CX,ZERO
LOOP2:NOP
       INCCX
       CMP CX,DELD
       JB LOOP2
       FPULSE
       FRDBYT BMD
       MOV CX,ZERO
LOOP3:NOP
       INCCX
       CMP CX,DELD
       JB LOOP3
       FPULSE
       FRDBYT BLO
       MOV CX,ZERO
LOOP4:NOP
       INCCX
       CMP CX,DELD
       JB LOOP4
       FPULSE
       ENDM
FTRANS MACRO            ; Translate 3 bytes to 2 for array.
       NOT    BHI      ; FTI is upside down.
       NOT    BMD
       NOT    BLO
       MOVAX,0
       MOV    AL,BHI
       MSIXAX
       MOVDX,0
       MOVDL,BMD
       ADD    AX,DX
       MSIXAX
       MOVDL,BLO
```

```
        ADD    AX,DX        ; AX = (BHI*64 + BMD)*64 + BLO
        MOV    ES:[BX],AX   ; Assume BX is the correct offset into the
        ENDM                ; given array.
        TITLE  FTILIB
        SUBTTL V0.0 10FEB88
        ; V0.1 18FEB88 - Try to use natural delay between
        ; FPULSE and read of BHI.
DATA    SEGMENT PUBLIC 'DATA'
HIBIT   EQU    1            ; Make strobe line +5V.
LOBIT   EQU    0            ; Make strobe line 0V.
        ; Note that usually the computer regards 1 as +5V and 0 as 0V.
        ; With our hacked printer board, the output for a 1 is 0V and for
        ; a 0 is +5V. Further along is a Schmidt Trigger which inverts these
        ; voltages back to the normal standard. They are then fed into the
        ; Fabritek Instrument which uses +5V as logical 0 and 0V as logical 1.
        ; The FTI wants the line to be normally logical 0 with a pulse to
        ; logical 1 and back to 0 to advance the memory address.
        ; Unfortunately the initial state of the computer is to feed 0V
        ; (logical 1) into the FTI (after the trigger). Thus the first
        ; transition the FTI sees is not a nice pulse, but a step from
        ; 0V to +5V (which is what the FTI triggers on).
        ; Now that is cleared up, on with the program!
ZERO    EQU0; A zero, just for general use
DELD    EQU5H; Number of NOPs for delaying the pulses
DPORT   EQU    278H         ; Hardwired address of data port on printer card.
CPORT   EQU    27AH         ; Hardwired address of control port.
BHI     DB     0            ; Most significant byte of the three.
BMD     DB     0            ;
BLO     DB     0
MAXN    DW     2*4096       ; Offset just past the end of the array.
ARENDDW0; Don't use MAXN - don't want to screw it up.
DATA    ENDS
DGROUP  GROUP  DATA
CODE    SEGMENT 'CODE'
        ASSUME CS:CODE,DS:DGROUP,SS:DGROUP
PUBLIC  FTIGET               ; Read spectrum.
PUBLIC  FTIHI                ; Strobe HI.
PUBLIC  FTILO                ; Strobe LO.
PUBLIC  FTIPLS               ; Pulse the stobe line - LO then HI.
PUBLIC  FTIRDT               ; Read the data port.
PUBLIC  FTIRCN               ; Read the control port.
PUBLICFTMEM; Read free disk space.
PUBLICFTKEY; Read keypress
FTIGET  PROC   FAR
        INTO
        LES    BX,DWORD PTR [BP+6]    ; Get pointer to the start of the
        MOVAX,BX; supplied array.
        ADDAX,MAXN
        MOVAREND,AX; AREND now points to end of array.
LOOP:   FREAD3
        CALLFTRNPC
        INC    BX
        INC    BX
        CMP    BX,AREND
        JBLOOP
        ; Data port now has 255(=0byte).
        ; Control port bit 0 now has a 1(=+5V).
        OUTOF
        RET    4
FTIGET  ENDP
FTRNPC  PROC   NEAR; Translate bytes to the array.
        PUSH   BP
        MOV    BP,SP
        FTRANS
        MOV    SP,BP
        POP    BP
        RET
FTRNPC  ENDP
```

```
FTIHI  PROC   FAR              ; Strobe HI, +5V.
       INTO
       MOV    DX,CPORT
       MOV    AX,HIBIT
       OUT    DX,AL
       OUTOF
       RET
FTIHI  ENDP
FTILO  PROC   FAR              ; Strobe LO, 0v.
       INTO
       MOV    DX,CPORT
       MOV    AX,LOBIT
       OUT    DX,AL
       OUTOF
       RET
FTILO  ENDP
FTIPLS PROC   FAR              ; Pulse the strobe line, LO to HI.
       INTO
       FPULSE
       OUTOF
       RET
FTIPLS ENDP
FTIRDT PROC   FAR              ; Read the data port.
       INTO
       LES    BX,DWORD PTR [BP+6]
       MOV    AX,0
       MOV    DX,DPORT
       IN     AL,DX
       MOV    ES:[BX],AX
       OUTOF
       RET    4
FTIRDT ENDP
FTIRCN PROC   FAR              ; Read the control port.
       INTO
       LES    BX,DWORD PTR [BP+6]
       MOV    AX,0
       MOV    DX,CPORT
       IN     AL,DX
       MOV    ES:[BX],AX
       OUTOF
       RET    4
FTIRCN ENDP
FTMEMPROCFAR; Find size of free disk space.
       INTO
       PUSHCX
       MOVAH,36H
       MOVDL,0
       INT21H
       MOVDX,BX
       LESBX,DWORD PTR [BP+14]
       MOVES:[BX],CX; Returns BytesPerSector in first parameter.
       LESBX,DWORD PTR [BP+10]
       MOVES:[BX],AX; SectorsPerCluster in second.
       LESBX,DWORD PTR [BP+6]
       MOVES:[BX],DX; NumberofFreeClusters in third.
       POPCX
       OUTOF
       RET12
FTMEMENDP
FTKEYPROCFAR; Read keypress.
       PUSHBP
       MOVBP,SP
       PUSHAX
       PUSHBX
       LESBX,DWORD PTR [BP+6]
       MOVAH,7
       INT21H
       MOVES:[BX],AL; Key in AL, or NUL and extended in AH.
       INCBX
       CMPAL,0
       JEEXTEN; If extended, get next keycode.
       MOVAL,0; If not, put 0 in low byte.
```

```
        JMPNEXTN
EXTEN:INT21H
NEXTN:MOVES:[BX],AL
        POPBX
        POPAX
        MOVSP,BP
        POPBP
        RET4
FTKEYENDP
CODE   ENDS
        END
```

7 Appendix B - The SMOOFT Subroutine (as used in data analysis)

(for a listing of the remainder of the SPEAK analysis package, see the Ph.D. thesis of M.H. Sidky [Si90])

```
c*********************************************************
      subroutine smooft(yin,n,pts)
c
c   smooths an array Yin of length N with a window whose
c   full width is of order PTS neighboring points, a user
c   supplied value.  Yin IS MODIFIED !!
c      Yin must fit inside y(2048), n+pts<=2048.
c
c*********************************************************
     implicit real*8 (a-h),(o-z)
      parameter(mmax=2048)
      dimension y(mmax),yin(mmax)
c************************
      do j=1,n
       y(j)=yin(j)
      end do
c************************
      m=2
      nmin=n+2.*pts
 1    if(m.lt.nmin)then
        m=2*m
      go to 1
      endif
c     write(*,*) 'n= ',n,' pts= ',pts,' m= ',m,' mmax= ',mmax
      if(m.gt.mmax) pause 'mmax too small. type CONTINUE to go on.'
      const=(pts/m)**2
      y1=y(1)
      yn=y(n)
      rm1=1./(n-1.)
      do 11 j=1,n
       y(j)=y(j)-rm1*(y1*(n-j)+yn*(j-1))
 11   continue
      if(n+1.le.m)then
       do 12 j=n+1,m
        y(j)=0
 12    continue
      endif
      mo2=m/2
      call realft(y,mo2,1)
      y(1)=y(1)/mo2
      fac=1.
      do 13 j=1,mo2-1
       k=2*j+1
       if(fac.ne.0.)then
        fac=dmax1(0.D0,((1.D0-const*j**2)/mo2))
        y(k)=fac*y(k)
        y(k+1)=fac*y(k+1)
       else
        y(k)=0.
        y(k+1)=0.
       endif
 13   continue
      fac=dmax1(0.D0,((1.D0-0.25*pts**2)/mo2))
      y(2)=fac*y(2)
      call realft(y,mo2,-1)
      do 14 j=1,n
       y(j)=rm1*(y1*(n-j)+yn*(j-1))+y(j)
 14   continue
c************************
      do j=1,n
       yin(j)=y(j)
      end do
c************************
      return
      end
```

```
c*************************************************************
      subroutine realft(data,n,imark)
c*************************************************************
      implicit real*8 (a-h),(o-z)
      real*8 wr,wi,wpr,wpi,wtemp,theta
      dimension data(2*n)
      REAL*16  h1i,h1r,h2i,h2r
         theta=3.141592653589793d0/dble(n)
         c1=0.5
         if (imark.eq.1) then
          c2=-0.5
          call four1(data,n,+1)
         else
          c2=0.5
          theta=-theta
         endif
         wpr=-2.0d0*dsin(0.5d0*theta)**2
         wpi=dsin(theta)
         wr=1.0d0+wpr
         wi=wpi
         n2p3=2*n+3
         do 11 i=2,n/2
          i1=2*i-1
          i2=i1+1
          i3=n2p3-i2
          i4=i3+1
          wrs=sngl(wr)
          wis=sngl(wi)
          h1r=c1*(data(i1)+data(i3))
          h1i=c1*(data(i2)-data(i4))
          h2r=-c2*(data(i2)+data(i4))
          h2i=c2*(data(i1)-data(i3))
          data(i1)=h1r+wrs*h2r-wis*h2i
          data(i2)=h1i+wrs*h2i+wis*h2r
          data(i3)=h1r-wrs*h2r+wis*h2i
          data(i4)=-h1i+wrs*h2i+wis*h2r
          wtemp=wr
          wr=wr*wpr-wi*wpi+wr
          wi=wi*wpr+wtemp*wpi+wi
 11      continue
         if (imark.eq.1) then
          h1r=data(1)
          data(1)=h1r+data(2)
          data(2)=h1r-data(2)
         else
          h1r=data(1)
          data(1)=c1*(h1r+data(2))
          data(2)=c1*(h1r-data(2))
          call four1(data,n,-1)
         end if
         return
         end
c*************************************************************
         subroutine four1(data,nn,imark)
c*************************************************************
      implicit real*8 (a-h),(o-z)
         real*8 wr,wi,wpr,wpi,wtemp,theta
         dimension data(2*nn)
         n=2*nn
         j=1
         do 11 i=1,n,2
          if(j.gt.i)then
            tempr=data(j)
            tempi=data(j+1)
            data(j)=data(i)
            data(j+1)=data(i+1)
            data(i)=tempr
            data(i+1)=tempi
          endif
          m=n/2
c 1       if ((m.ge.2).and.(j.gt.m)) then
         DO WHILE((M.GE.2).AND.(J.GT.M))
           j=j-m
```

```
          m=m/2
C         go to 1
C         endif
        END DO
          j=j+m
11      continue
        mmax=2
2     if (n.gt.mmax) then
          istep=2*mmax
          theta=6.28318530717959d0/(imark*mmax)
          wpr=-2.d0*dsin(0.5d0*theta)**2
          wpi=dsin(theta)
          wr=1.d0
          wi=0.d0
          do 13 m=1,mmax,2
            do 12 i=m,n,istep
              j=i+mmax
              tempr=sngl(wr)*data(j)-sngl(wi)*data(j+1)
              tempi=sngl(wr)*data(j+1)+sngl(wi)*data(j)
              data(j)=data(i)-tempr
              data(j+1)=data(i+1)-tempi
              data(i)=data(i)+tempr
              data(i+1)=data(i+1)+tempi
12          continue
            wtemp=wr
            wr=wr*wpr-wi*wpi+wr
            wi=wi*wpr+wtemp*wpi+wi
13        continue
          mmax=istep
        go to 2
        endif
        return
        end
```